

AD-A179 670

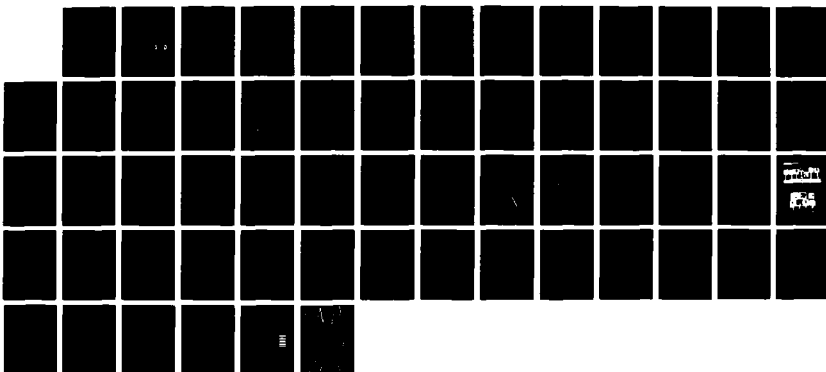
DESIGN OF NON-DISCRETE DIAPHRAGM PRESSURE GAGE FOR
BLAST PRESSURE MEASUREMENTS(U) ARMY BALLISTIC RESEARCH
LAB ABERDEEN PROVING GROUND MD H J GOODMAN ET AL
MAR 87 BRL-TR-2783

1/1

UNCLASSIFIED

F/G 14/2

ML





MI

AD

AD-A179 670

TECHNICAL REPORT BRL-TR-2783

DESIGN OF NON-DISCRETE DIAPHRAGM
PRESSURE GAGE FOR BLAST PRESSURE
MEASUREMENTS

HENRY J. GOODMAN
EVAN H. WALKER
EMMETT L. BELL

MARCH 1987

DTIC
ELECTE
APR 29 1987
S D

APPROVED FOR PUBLIC RELEASE; DISTRIBUTION UNLIMITED.

US ARMY BALLISTIC RESEARCH LABORATORY
ABERDEEN PROVING GROUND, MARYLAND

Destroy this report when it is no longer needed.
Do not return it to the originator.

Additional copies of this report may be obtained
from the National Technical Information Service,
U. S. Department of Commerce, Springfield, Virginia
22161.

- The findings in this report are not to be construed as an official
Department of the Army position, unless so designated by other
authorized documents.

The use of trade names or manufacturers' names in this report
does not constitute indorsement of any commercial product.

UNCLASSIFIED

SECURITY CLASSIFICATION OF THIS PAGE

AD-A177

REPORT DOCUMENTATION PAGE

Form Approved
OMB No 0704-0188
Exp. Date Jun 30, 1986

1a. REPORT SECURITY CLASSIFICATION UNCLASSIFIED		1b. RESTRICTIVE MARKINGS	
2a. SECURITY CLASSIFICATION AUTHORITY		3. DISTRIBUTION/AVAILABILITY OF REPORT Approved for public release; distribution is unlimited.	
2b. DECLASSIFICATION/DOWNGRADING SCHEDULE			
4. PERFORMING ORGANIZATION REPORT NUMBER(S) BRL-TR-2783		5. MONITORING ORGANIZATION REPORT NUMBER(S)	
6a. NAME OF PERFORMING ORGANIZATION USA Ballistic Research Laboratory	6b. OFFICE SYMBOL (If applicable) SLCBR-VL-S	7a. NAME OF MONITORING ORGANIZATION	
6c. ADDRESS (City, State, and ZIP Code) USA Ballistic Research Laboratory Aberdeen Proving Ground, MD 21005-5066		7b. ADDRESS (City, State, and ZIP Code)	
8a. NAME OF FUNDING/SPONSORING ORGANIZATION	8b. OFFICE SYMBOL (If applicable)	9. PROCUREMENT INSTRUMENT IDENTIFICATION NUMBER	
8c. ADDRESS (City, State, and ZIP Code)		10. SOURCE OF FUNDING NUMBERS	
		PROGRAM ELEMENT NO.	PROJECT NO.
		TASK NO.	WORK UNIT ACCESSION NO.
11. TITLE (Include Security Classification) Design of Non-Discrete Diaphragm Pressure Gage for Blast Pressure Measurements			
12. PERSONAL AUTHOR(S) Henry J. Goodman, Evan H. Walker, Emmett L. Bell			
13a. TYPE OF REPORT Technical	13b. TIME COVERED FROM TO	14. DATE OF REPORT (Year, Month, Day) March 1987	15. PAGE COUNT 55
16. SUPPLEMENTARY NOTATION A diaphragm peak pressure gage has been designed. I +			
17. COSATI CODES		18. SUBJECT TERMS (Continue on reverse if necessary and identify by block number)	
FIELD	GROUP	SUB-GROUP	
		Diaphragm Gage Blast Measurement	
		Foil Gage Quasi-Static Pressure	
		Blast Overpressure	
19. ABSTRACT (Continue on reverse if necessary and identify by block number)			
<p>A diaphragm peak pressure gage that provides a convenient and inexpensive method to measure the peak overpressure due to explosion in air, or other forms of pressure transients, occurring too rapidly to be recorded by a static pressure measuring device has been designed. A diaphragm pressure gage to measure the maximum quasi-static overpressure inside an enclosure has also been designed.</p> <p>The overall sizes of these gages are convenient and practical, and provide a distinctive mechanism whereby the peak overpressure can be read directly from a graduated scale or continuous readings can be obtained with a depth gage.</p> <p>These gages are ideally suited to yield accurate and reliable peak overpressure readings over a wide pressure range in hazardous environments presented by explosives where electronic pressure transducers are not available, the environment is not conducive to the</p>			
20. DISTRIBUTION/AVAILABILITY OF ABSTRACT <input type="checkbox"/> UNCLASSIFIED/UNLIMITED <input checked="" type="checkbox"/> SAME AS RPT. <input type="checkbox"/> DTIC USERS		21. ABSTRACT SECURITY CLASSIFICATION UNCLASSIFIED	
22a. NAME OF RESPONSIBLE INDIVIDUAL HENRY J. GOODMAN		22b. TELEPHONE (Include Area Code) (301) 278-6290	22c. OFFICE SYMBOL SLCBR-VL-S

19. Abstract:

(a)
use of electronic devices or where ~~the~~ back-up measuring device is desired to ensure a reading in the event of electronic device failure.

The transient diaphragm pressure gage can be calibrated to yield overpressure readings so that spurious effects such as voltage surges or fragment impacts on the gages, effects that are not caused by the pressure pulse itself, cannot yield false readings. This gage when calibrated is less sensitive to the pulse shape than prior diaphragm gages and can be calibrated to measure side-on or face-on peak shock overpressures. *Keywords.*

Foil gages; Blast overpressure measurement. *A*

TABLE OF CONTENTS

	LIST OF ILLUSTRATIONS.....	iv
I	INTRODUCTION.....	1
II	OBJECTIVE.....	4
III	GAGE CHARACTERISTICS.....	4
IV	CALIBRATION.....	9
V	RESULTS.....	11
VI	CONCLUSION.....	32
	REFERENCES.....	37
	APPENDIX - EQUATIONS.....	39
	LIST OF SYMBOLS.....	49
	DISTRIBUTION LIST.....	51



Accession For	
NTIS CRA&I	<input checked="" type="checkbox"/>
DTIC TAB	<input type="checkbox"/>
Unannounced	<input type="checkbox"/>
Justification	
By	
Distribution /	
Availability Codes	
Dist	Avail and/or Special
A-1	

LIST OF ILLUSTRATIONS

1	Plan view of the Combat Systems Testing Activity gage and its construction.....	2
2	Plan view of the Surface Mounted Discrete Diaphragm Pressure Gage (SMDDPG) and its construction.....	5
3a	Plan and end view of the Non-Discrete Diaphragm Pressure Gage (NDDPG).....	7
3b	Construction of the (NDDPG).....	7
4a	Plan and end view of the Quasi-Static Diaphragm Pressure Gage (QS-DPG).....	8
4b	Construction of QA-DPG.....	8
5	Typical side-on pressure-time profile measured with electronic transducer in the 24 inch shock tube.....	10
6	Calibration curves for the NDDPG with .0005 inch aluminum foil oriented face-on to the propagating shock.....	12
7	Calibration curves for NDDPG with .001 inch aluminum foil oriented face-on to the propagating shock.....	13
8	Calibration curves for NDDPG with .003 inch aluminum foil oriented side-on, face-on, 10 degree incident and 30 degree incident to the propagating shock.....	15
9	Calibration curves for NDDPG with .005 inch aluminum foil oriented face-on and side-on to the propagating shock.....	16
10	Calibration curves for the SMDDPG and the CSTA gage with .0005 inch foil oriented side-on and face-on to the propagating shock...	17
11	Calibration curves for SMDDPG 1 1/2 inch diameter and 3/4 inch diameter diaphragms oriented face-on to propagating shock.....	20
12a	Pressure-time history for 8 pounds of pentolite with a Pmax of 3.7 psi.....	22
12b	Pressure-time history for 8 pounds of pentolite with a Pmax of 19.4 psi.....	22
13a	Pressure-time history for 8 pounds of pentolite with a Pmax of 14.2 psi.....	23
14a	Pressure-time history for 8 pounds of pentolite with a Pmax of 26.7 psi.....	24

LIST OF ILLUSTRATIONS (continued)

14b	Pressure-time history for 8 pounds of pentilite with a Pmax of 45.1 psi.....	24
15	Pressure-time history for 8 pounds of pentolite with a Pmax of 64.0 psi.....	25
16	Calibration curves for QS-DPG.....	26
17	Reflected overpressure versus side-on overpressure.....	28
18	Side-on overpressure versus side-on impulse for 8 pounds of pentolite.....	29
19	Side-on overpressure versus side-on duration for 8 pounds of pentolite.....	30
20	Side-on impulse versus side-on duration for 8 pounds of pentolite.....	31
21	Diaphragm pressure gages after compartment test.....	33
22	Diaphragm pressure gages after compartment test.....	33

I. INTRODUCTION

Diaphragm pressure gages provide a convenient and inexpensive method to measure peak blast overpressure. These devices are frequently employed where electronic transducers are not available, the environment is not conducive to the use of electronic transducers, or where a backup system to measure peak overpressure is desirable.

As with all types of pressure gages, there exists the problem of achieving repeatability and reliability. The requirements for achieving repeatability and reliability with diaphragm or foil gages were established through the work of Read¹ at Princeton. These tests were conducted with Ballistic Research Laboratories (BRL) type blast gages. Figure 1 shows a Combat Systems Testing Activity (CSTA) gage, which is an example of the diaphragm gage. For the proper use of this gage it is necessary to determine the following:

1. selection of diaphragm material
2. calibration procedures
3. dependence of critical or rupture pressure on wave form
4. dynamic reloading effects
5. static load effects
6. apparatus procedure.

The BRL type gage contained a series of circular diaphragms. Pressure readings with this gage were indicated by the largest diaphragm ruptured, and the smallest diaphragm that failed to rupture. A discrete rupture pressure or critical pressure exists for each diaphragm diameter. A ruptured diaphragm records a pressure interval, the lower limit being the rupture pressure of the diaphragm under consideration and the upper limit, the discrete rupture pressure of the next smaller diaphragm. Hence, instead of continuous pressure readings, the actual pressure is only bracketed. The pressure range bracketed depends on the diameters and the number of diaphragms in the gage housing. As a consequence, this type of pressure gage is quite limited in its utility.

BRL has developed a new diaphragm gage that retains the simplicity and repeatability of previous diaphragm type gages, but provides a continuous scale for pressure readings. This gage called "Non-Discrete Diaphragm Pressure Gage (NDDPG)," has not only the advantages, simplicity, and ruggedness of the old gages developed at BRL and refined at Princeton, but also, these gages avoid such problems as artificial

¹Read, W.T.; "Calibration and Use of Diaphragm Blast Meters," NDRC Report No. A392 (OSRD Report No. 6363), Division 2, National Defense Research Committee, Washington, D.C., 1945.

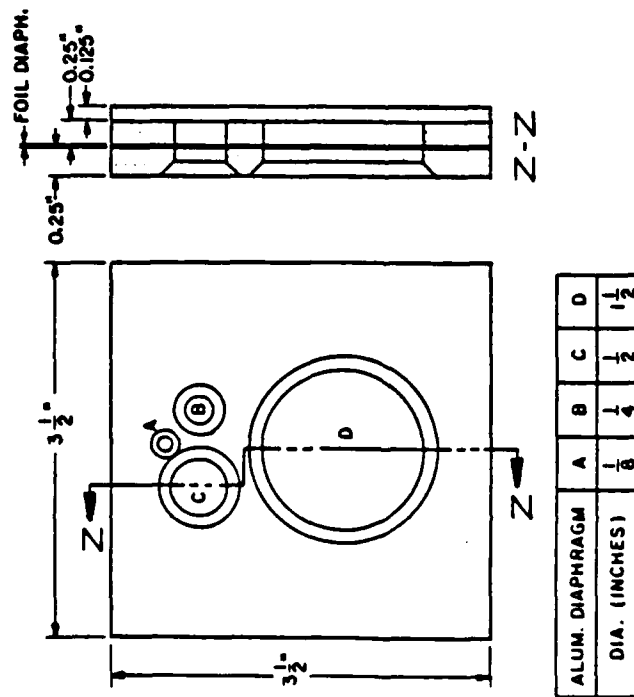
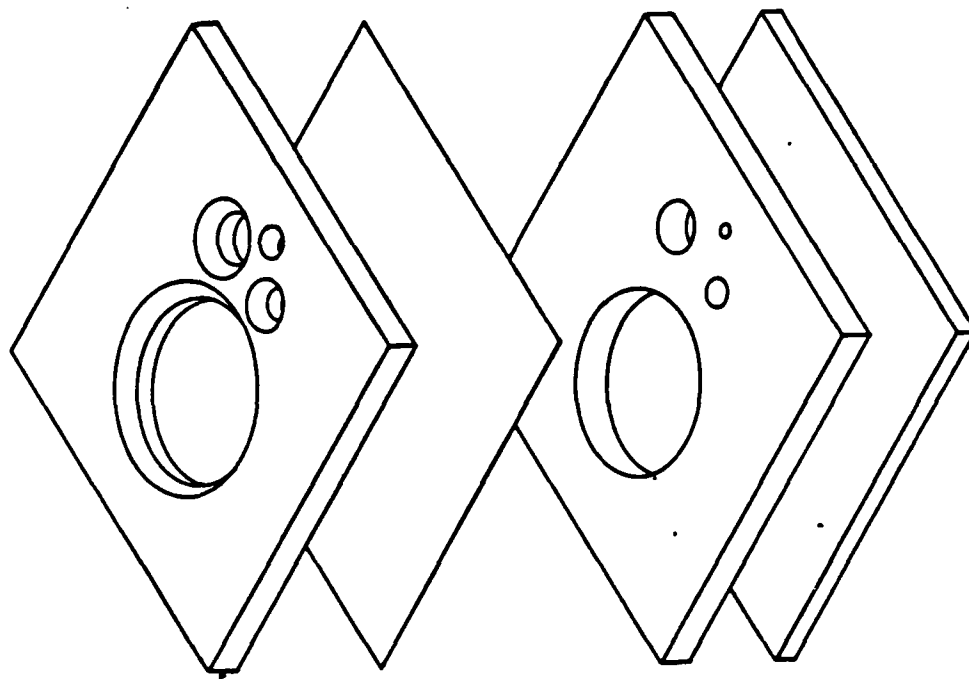


Figure 1. Plan view of the Combat Systems Testing Activity gage and its construction.

pressure readings (spurious electronic spikes) or loss of signal due to broken lead-in wires to electronic devices. When the central question to be answered is "what is the peak effective pressure (i.e., ignoring exceedingly brief transients that do not produce effects on men or equipment) exerted in the test environment?" the gage can provide dependable information.

Unlike prior mechanical gages, this NDDPG has proved to give accurate peak overpressure readings that appear to be less dependent on the incident pressure pulse shape.

To explain the operations of these new continuous reading diaphragm pressure gages, we need to consider, in detail, how the conventional gages work. The tests at Princeton showed that a metallic diaphragm of pure annealed aluminum foil is best for providing uniform test results, and the initial pressure pulse produces the maximum deformation or causes the diaphragm to rupture. Small subsequent shock pressure wave reflections have an insignificant effect. The effect requiring significantly higher reflected pressures to increase permanent deformation to a diaphragm, concave to the direction in which the wave propagates, is due to the fact that the diaphragm is strengthened when the initial shock deforms it.²

The Princeton study also showed that the maximum deformation or rupture pressure depends on wave form. When step waves generated by a shock tube were used to calibrate the gages, pressures recorded from small charges having wave forms that could be expressed with an exponential function or waves that decayed rapidly, had to be 10% to 20% higher in order to rupture the same size diameter diaphragms. The diaphragm surface was recessed in its housing and the wave front direction of propagation was normal to the diaphragm surface. Hence, face-on pressures or normally reflected pressures were measured. At Operation Greenhouse³ (a nuclear blast trial), a surface mount discrete diaphragm pressure gage (SMDDPG) with foil at the surface rather than being recessed was used to measure side-on pressure. The direction of travel of the blast wave was parallel to the foil surface, hence side-on pressure. There were no significant differences in the maximum pressure measurements by the foil gages and those measured by electronic transducers.

²Dresner, Lawrence; "Motion Of Elasto-Plastic Membranes Under Shock Loading," Journal of Applied Physics, Volume 41, No. 5, 1970.

³Meszaros, Julius; "Determination of Mach Region Blast Pressure with Foil Meters," Operation Greenhouse, Scientific Director Report WT-55, Annex 1.6, Part III, Section 2, Ballistic Research Laboratories, Aberdeen Proving Ground, MD, 1951 (C).

A non-rupturing diaphragm gage has also been developed that determines the peak overpressure to an accuracy of 10%.⁴ Even though this gage has circular diaphragms, it gives a continuous pressure reading from the correlation of maximum deformation and pressure as long as the diaphragm does not rupture. However, the total continuous peak overpressure range of this gage is less than that of the new NDDPG.

II. OBJECTIVE

The objective of this work was to develop an inexpensive diaphragm type gage, requiring minimal time for set-up in test situations, with reliable, repeatable, continuous (non-discrete) overpressure readings with or without rupture of the diaphragm.

III. GAGE CHARACTERISTICS

The size of all gages discussed in this work is constrained to approximate the size of the foil gage used by the CSTA at Aberdeen Proving Ground, MD. Figure 1 depicts the CSTA type gage. A rupture type gage (discrete pressure measurements), with the diaphragm mounted at the gage housing surface, instead of being recessed was fabricated and is shown in Figure 2. This gage which was called the surface mounted discrete diaphragm pressure gage (SMDDPG) had more diaphragms than the CSTA gage, thus increasing the number of pressure intervals and decreasing the range of each pressure interval.

The final permanent shape of the ductile diaphragm material after blast loading is well defined, and when rupture occurs several variations of a single crack without branches occur for circular diaphragms.^{5,6} For the NDDPG, a diaphragm material of pure annealed aluminum, 99.4% pure, with negligible elastic effects (elastic limit occurs at negligibly small strain) was selected. This material is such.

⁴Manweiler, R.W.; Chester, C.V.; and Kearney, C.H.; "Measurements of Shock Over-Pressures in Air by a Yielding Foil Membrane Blast Gage," ORNL Report 4863, Oak Ridge National Laboratory, Oak Ridge, Tennessee, September 1973.

⁵Hudson, G.E.; "A Theory of the Dynamic Deformation of a Thin Diaphragm," Journal Of Applied Physics, Volume 22, No. 1, January 1951.

⁶Sachs, George; Epsey, George; and Kasik, G.P.; "Circular Bulging of Aluminum-Alloy Sheets at Room and Elevated Temperature," ASME, January-December 1946.

DIAPHRAGM INSERTS

ALUM. DIAPHRAGM	A1	A2	B1	B2	C1	C2	C3	C4	C5	C6
DIAMETER (IN.)	$1\frac{1}{2}$	1	$\frac{3}{4}$	$\frac{1}{2}$	$\frac{3}{8}$	$\frac{1}{4}$	$\frac{3}{16}$	$\frac{1}{8}$	$\frac{3}{32}$	$\frac{1}{16}$

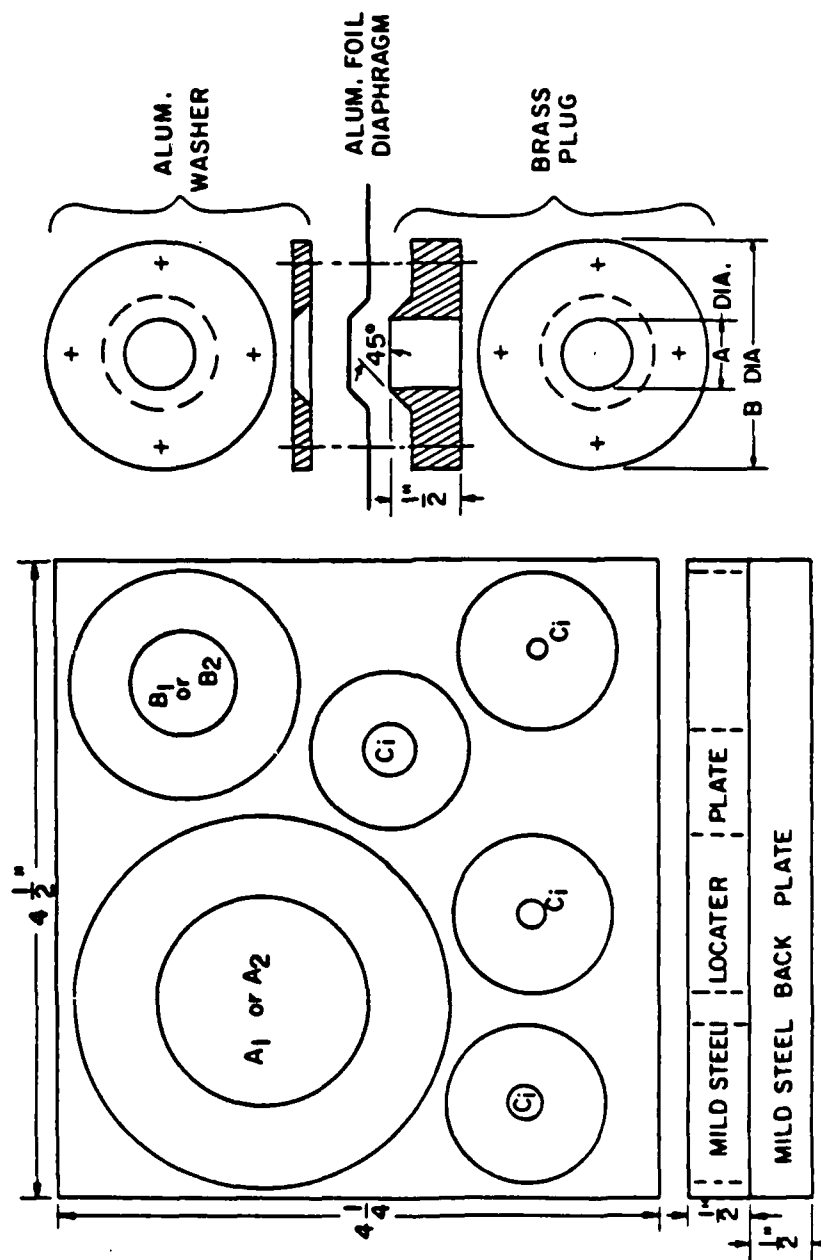


Figure 2. Plan view of the Surface Mounted Discrete Diaphragm Pressure Gage (SMDDPG) and its construction

that strain rate does not affect the flow for the finite deformation and strains considered. A cone-shaped gage design was selected to control the direction of the crack when the foil ruptured (see Figures 3a and 3b). This gage combines the features of a yielding diaphragm gage without rupture, and a gage where pressures were determined by the rupture length in the diaphragm. In the case of non-rupture, the peak overpressure is determined from the maximum depth of the diaphragm deformation. For rupture, the crack or ruptured area propagated in the direction of the cones axis and the length of the crack or rupture area is used to determine the peak overpressure. These peak overpressures are read off a calibrated scale on the front of the gage housing, for the rupture case. In the case of non-rupture, the accuracy is dependent upon the accuracy with which one measures the maximum foil deformation. If the foil ruptures, the pressure measurements are not as accurate because of the scatter in the length measurements of the rupture crack or rupture area that are read from the scale on the gage housing. Nevertheless, good peak overpressure measurements can be obtained. In both cases, rupture or non-rupture, the readings are non-discrete; thus providing a NDDPG or continuous reading diaphragm pressure gage.

International Foil of Alliance, Ohio supplied the diaphragm materials for the NDDPG which was 1145-0 annealed aluminum foil, 99.4% pure in thicknesses of .0005 inch, .001 inch, .003 inch, and .005 inch. Initial tests showed that a knife located behind the foil, at the center of the maximum diameter of the cavity, shown in Figure 3a, caused rupture to occur after a small deformation. The length could be read directly from a scale on the housing. The foil puncture knife had two sharp edges aligned along the cone axis and came to a point at its upper end. Because of the gage size constraint, the pressure range of this version of the NDDPG gage was short and not adequate for most of the field tests for which it was designed.

The gage shown in Figures 3a and 3b without a knife, utilizing deformation, and rupture characteristics was adopted as the most reliable and accurate gage for measuring the face-on peak overpressure of a fast rising transient pulse with blast or shock wave characteristics. A 3/4 inch cavity behind the foil was used so that natural rupture could occur before the deforming foil reached the bottom of the cavity. In order to keep the foil from being cut along the cavity edge at high pressures, the edge of the cavity adjacent to the foil had a 1/32 inch by 45 degree chamfer.

Figures 4a & 4b show a variation of the NDDPG gage, the quasi-static diaphragm pressure gage (QS-DPG) designed to measure the peak overpressure of a slow rising pulse generated due to some source of heat energy in an enclosure. This quasi-static pressure was measured by creating two cavities separated by the foil, and allowing the hot gases to enter the front cavity through a shock attenuation tube, located at the small end of the cavity. The entrance to the front cavity of the

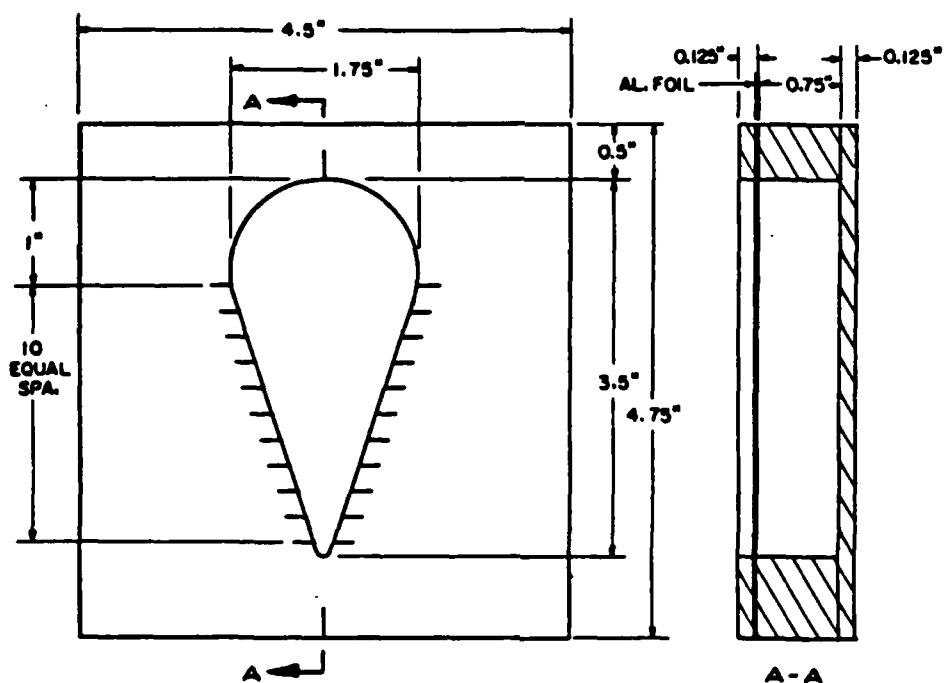


Figure 3a. Plan and end view of the Non-Discrete Diaphragm Pressure Gage (NDDPG)

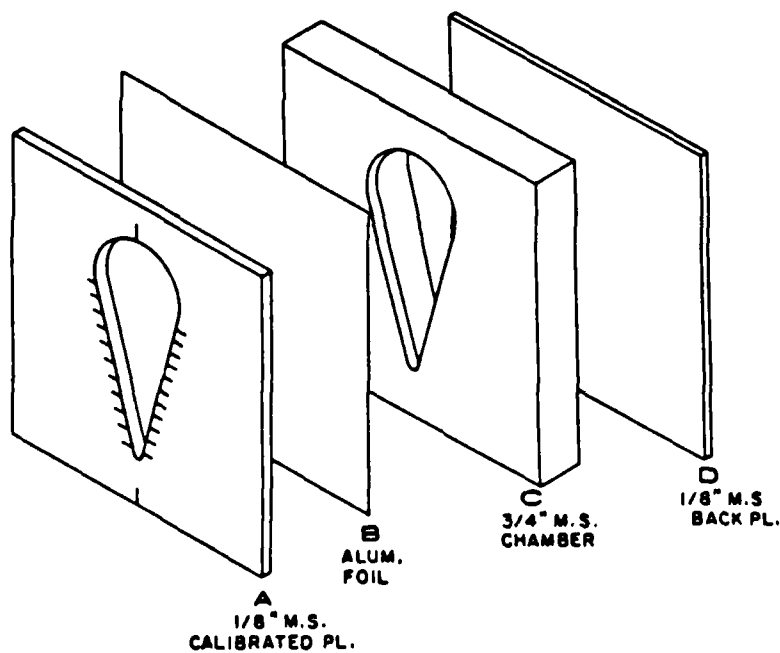


Figure 3b. Construction of the (NDDPG)

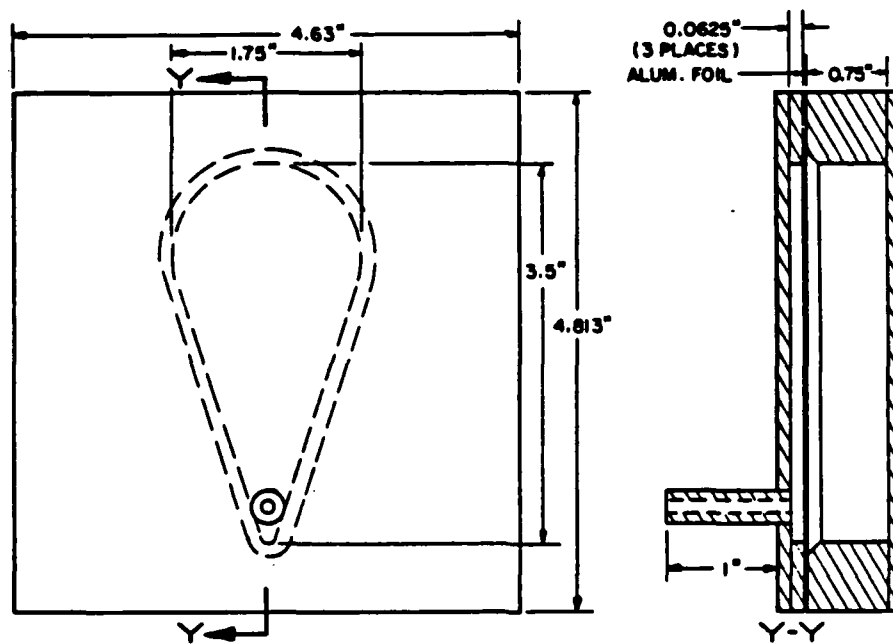


Figure 4a. Plan and end view of the Quasi-Static Diaphragm Pressure Gage (QS-DPG)

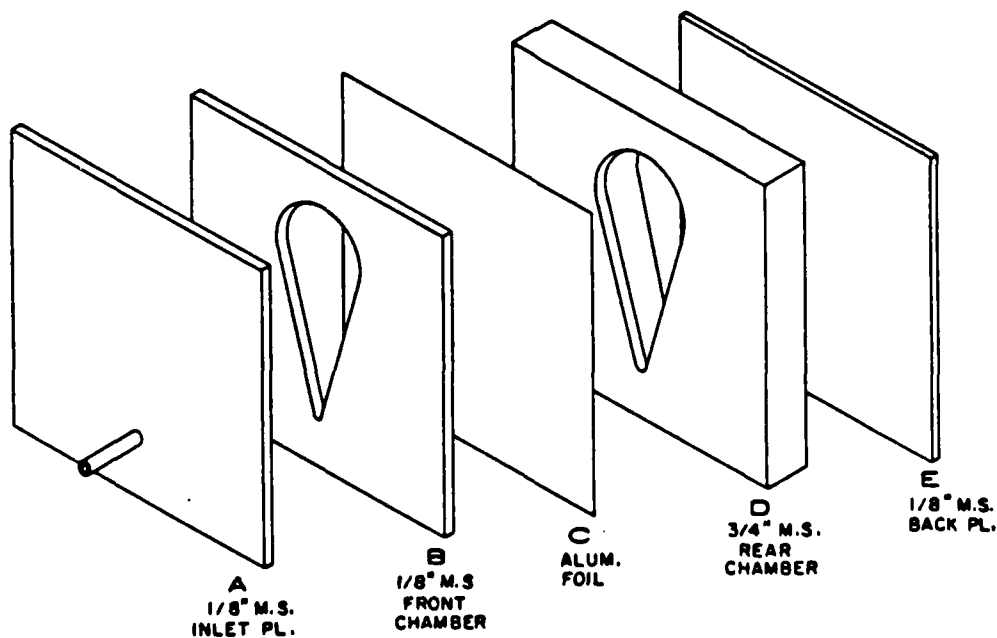


Figure 4b. Construction of QS-DPG

gage was positioned so that if shocks entered, the foil deformation at this point would be minimal and the maximum deformation would occur at the large diameter, because of the high pressure gas or quasi-static pressure buildup. Plates A and B, of Figure 4b are welded together to form the entrance cavity and plates D and E were welded together to form the rear cavity of the gage. The foil C, in Figure 4b was placed over the cavity in plate D with an adhesive sealant (Silastic 722RTV). Figure 4a shows the front and side views of the assembled gage.

IV. CALIBRATION

The 99.4% pure annealed aluminum metallic diaphragm material was calibrated in the BRL 24 inch open end shock tube (ST) and later in field experiments using eight pound spherical pentolite charges fired near the ground so that measurements could be made in the Mach stem region. For the shock tube tests, the foil in the NDDPG gage housing was mounted in the center of the ST tube and oriented so that the shock wave impacted side-on (90 degree incident angle), 30 degree incident angle, 10 degree incident angle, and face-on or normally reflected (0 degree incident angle). The angle of incidence is defined as the angle between the shock front normal and the normal to an impacted surface. Hence, side-on orientation is that in which the plane of the foil in the gage housing is parallel to the direction of propagation of the shock, and the shock travels across the face of the gage with a finite velocity. Face-on or normally reflected measurements were made when the orientation of the foil in the gage was such that its plane was perpendicular to the direction in which the shock propagated, and the shock impacted the foil surface at all points simultaneously.

In order to keep the enveloping shock from affecting the foil from the rear of the gage cavity, the cavity behind the foil was closed. A small hole was placed in plate D of Figure 3b so that the barometric pressure and temperature changes would not change the maximum permanent deformation for a given pressure level. In these tests it was found that the maximum deformation depth was the same at the shock pressure levels tested with or without the hole. However, for .0005 inch foil the permanent maximum deformation depth was not smooth with the hole in the cavity.

The peak side-on overpressure at the NDDPG gage location in the shock tube was measured with a Piezotronic PCB type 1134A24 quartz piezoelectric electronic transducer. Figure 5 is a typical pressure time trace. The side-on and face-on pressures were also computed from

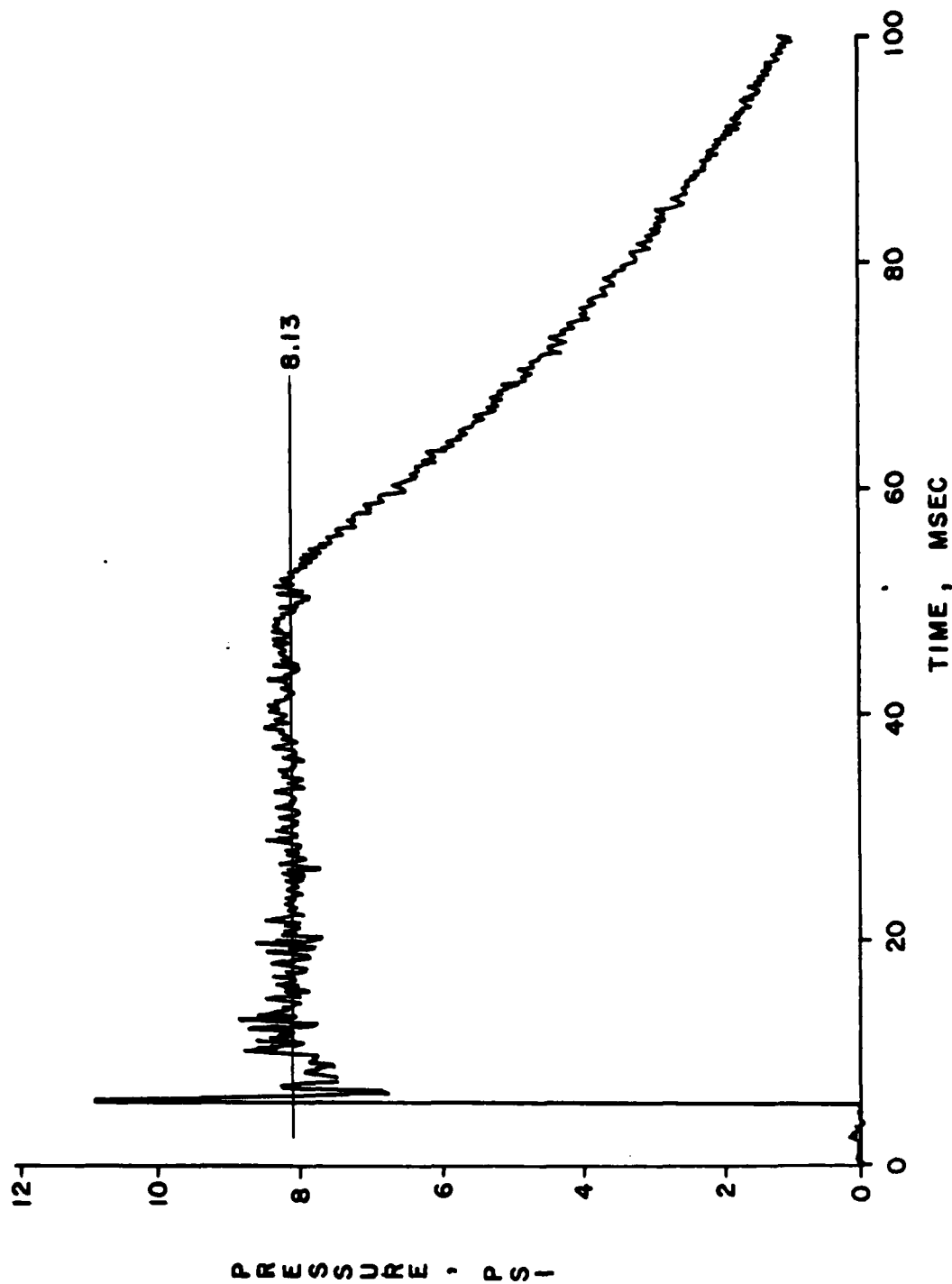


Figure 5. Typical side-on pressure-time profile measured with electronic transducer in the 24 inch shock tube.

the gas properties in the shock tube. The recorded pressures, corresponding to the deformation or rupture experienced by the foil, were the average values of the side-on pressures measured by the PCB gage and those computed from the gas properties in the shock tube.

Maximum permanent deformation depth occurred in the large diameter of the NDDPG foil gage, and this depth was measured with a depth micrometer gage having a base and measuring rod with .001 inch graduations. The zero of the rupture scale on the gage housing was the mark at maximum diameter. This mark represents the minimum pressure needed to cause rupture and at this point rupture begins. It should be noted that it was impossible to determine a single rupture pressure and there is a discontinuity or transition region in the immediate vicinity of the rupture point. A similar condition occurs for electronically measured shock pressures when the ratio of local flow velocity and local sound velocity behind the shock is one.⁷ The scale on the gage housing is read from the initial scale mark at the maximum opening (cone base) toward the vertex of the cone. The length of the rupture was defined as the rupture length in the direction of the cone axis beginning at the initial scale mark. In many instances the ruptures were elliptical and the lengths were along the major axis beginning at the initial mark of the rupture scale.

V. RESULTS

LSPLOT-CDC VERSION, an interactive data plotting and analysis program for use with the Tektronix graphic terminals, has been used to plot and analyze the experimental data. Computer drawn curves are presented in Figures 6 through 11, and Figures 16 thru 20 showing the data points, together with least square fitted polynomial curves, to serve as pressure calibration curves.

Even though the gage may or may not have been oriented side-on, the pressure data was converted to peak side-on overpressures because this was the pressure of interest in the project. These side-on overpressures were those measured electronically or computed for the calibration orientation. Figures 6 and 7 give the overpressure versus permanent deformation, and overpressure versus rupture length for .0005 and .001 inch foil mounted in the NDDPG when impacted face-on by a shock. In these tests each scale mark shown on plate A of Figure 3b is a unit of length measurement and the mark at maximum diameter is the initial

⁷ Goodman, Henry J.; "Aerodynamic and Frequency Dependent Errors in Air Blast Gages," BRL Report 1345, Ballistic Research Laboratories, Aberdeen Proving Ground, MD, October 1966.

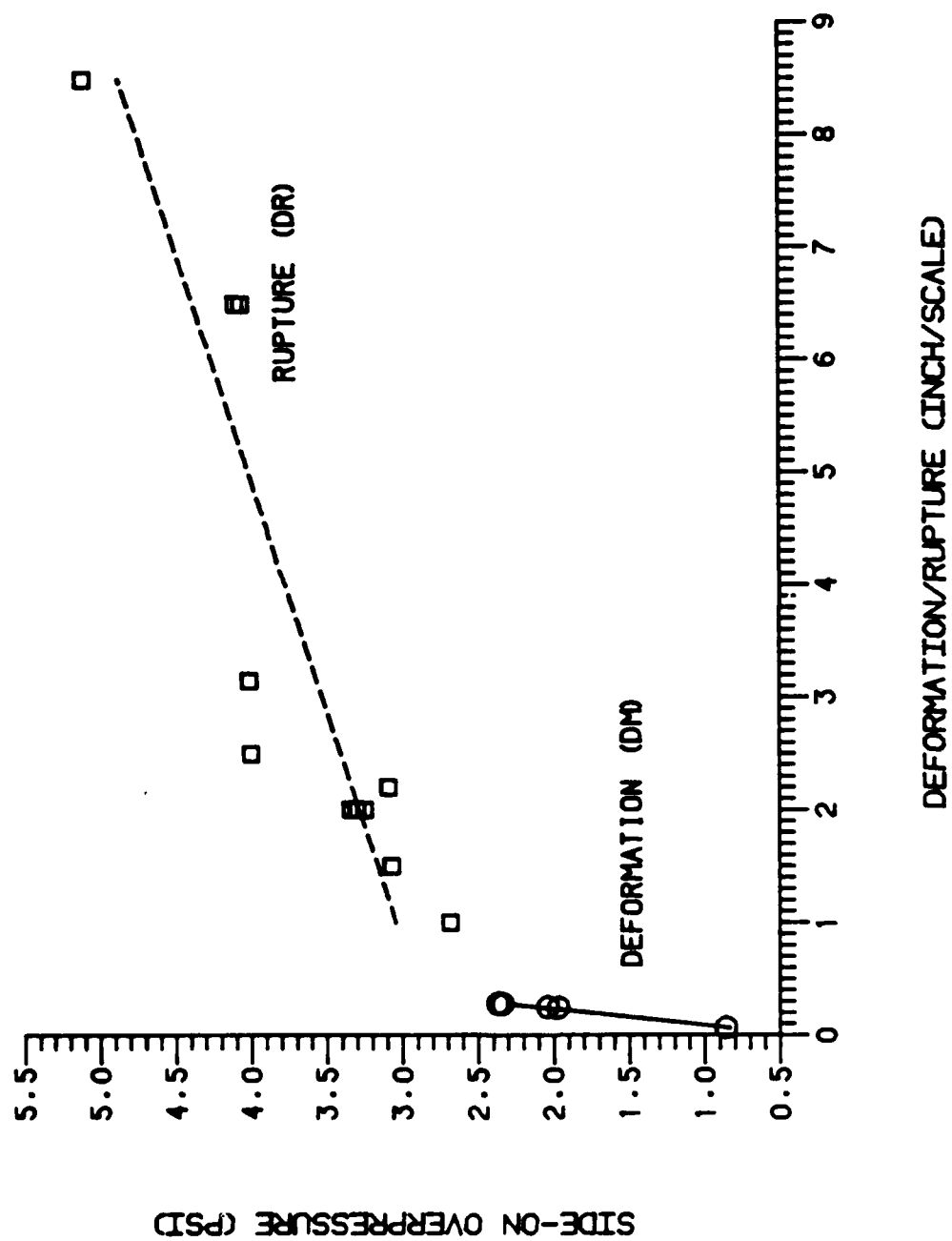


Figure 6. Calibration curves for the NDDPG with .0005 inch aluminum foil oriented face-on to the propagating shock

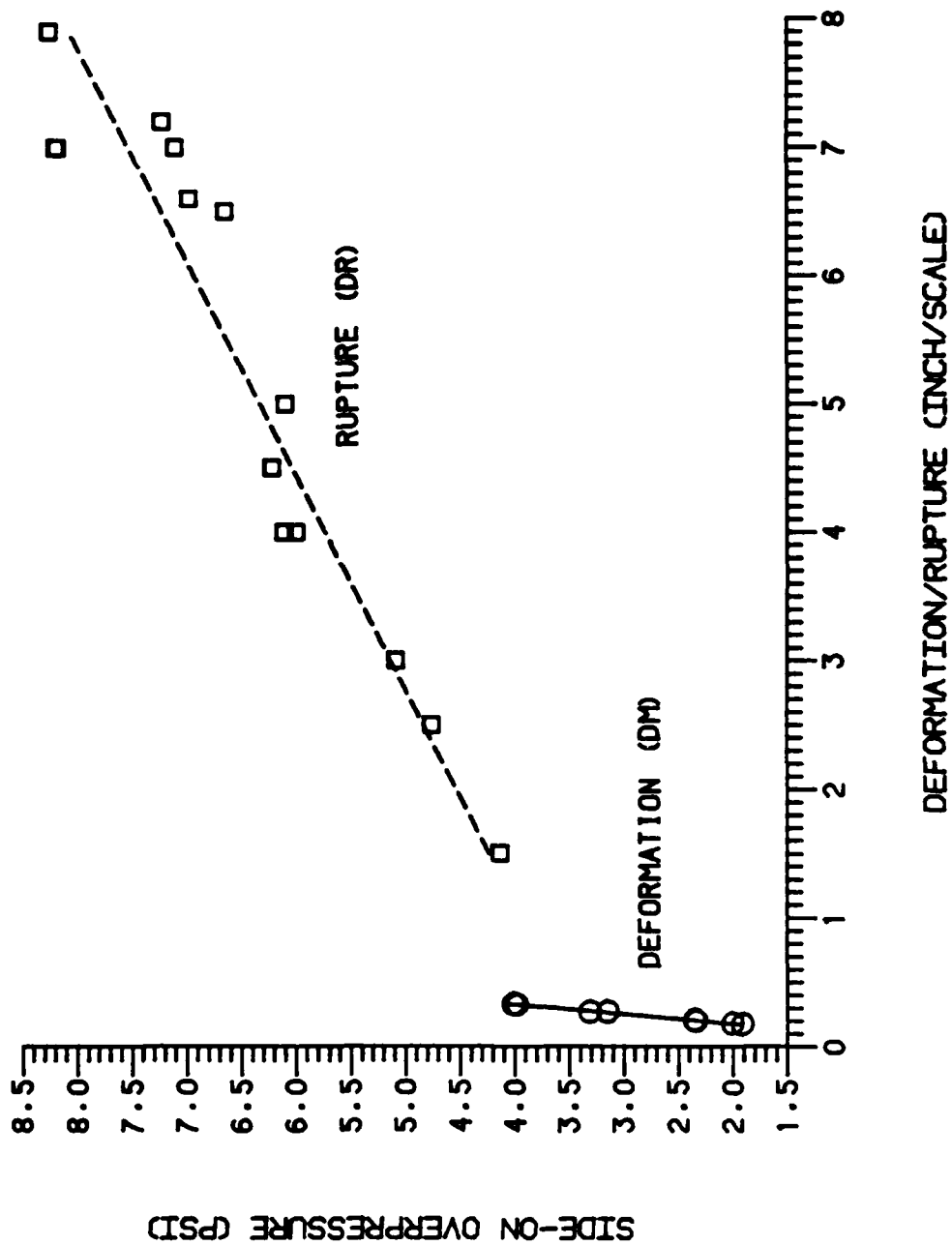


Figure 7. Calibration curves for NDDPG with .001 inch aluminum foil oriented face-on to the propagating shock

point. The plots show a transition region between the maximum point of foil deformation and the minimum point of rupture on the rupture scale and an extrapolation should not be made in this transition region.

The steel mounting shaft used to insert the gage housing into the shock tube was not adequate to withstand pressures required to determine the rupture scale pressures for .003 and .005 inch aluminum foil. However, the range of pressures determined from the maximum deformation depths were sufficient for the field tests in which the gage was to be used. Attempts to extend the range of pressures into the rupture region for these two thicknesses were discontinued, because the mounting shaft began to bend at the high pressures.

Figure 8 is the pressure versus maximum deformation for .003 inch foil mounted in the NDDPG when oriented side-on (90 degree incident angle), at 10 degree incident angle, at 30 degree incident angle, and face-on (0 degree incident angle). The solid line is for face-on (ST), long dash for face-on (EXPL), dot for 10 degree, short dash for 30 degree, and dash for side-on (ST and EXPL). This Figure shows that at 10 degrees and 30 degrees the pressure deviation is not significantly different from face-on pressure measurements. For side-on pressure, an order of magnitude increase in pressure is needed to produce the same permanent deformation as a wave impacting face-on. This Figure can be used to determine the peak overpressure when side-on pressures are desired. For a small angle of misalignment, the gage will give good face-on pressure measurements.

Figure 9 is the pressure versus maximum deformation for the .005 inch foil mounted in the NDDPG when oriented face-on and side-on. The solid line is for face-on (ST) and the dotted line is for face-on (EXPL).

Figure 10 is a plot of the rupture pressures for the CSTA type gage and the SMDDPG. The SMDDPG measurements were made at face-on and side-on orientation. This figure shows that an order of magnitude increase in side-on overpressure must exist in order to have similar diameter diaphragms that ruptured face-on to rupture side-on. These gages give discrete pressure ranges for ruptured diaphragms and these values are given in Table 1 for the CSTA type gage and Table 2 for the SMDDPG.

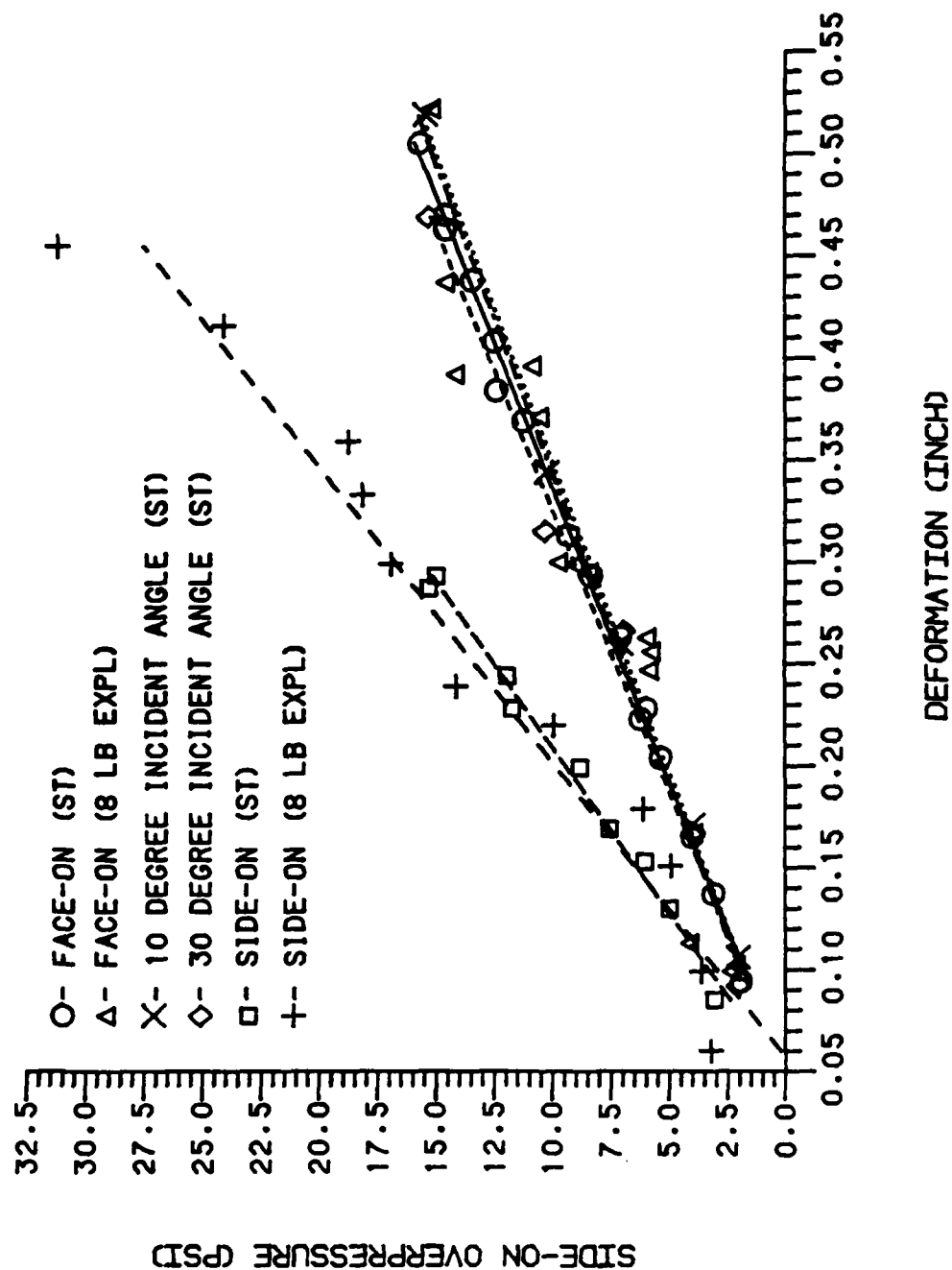


Figure 8. Calibration curves for NDDPG with .003 inch aluminum foil oriented side-on, face-on, 10 degree incident and 30 degree incident to the propagating shock

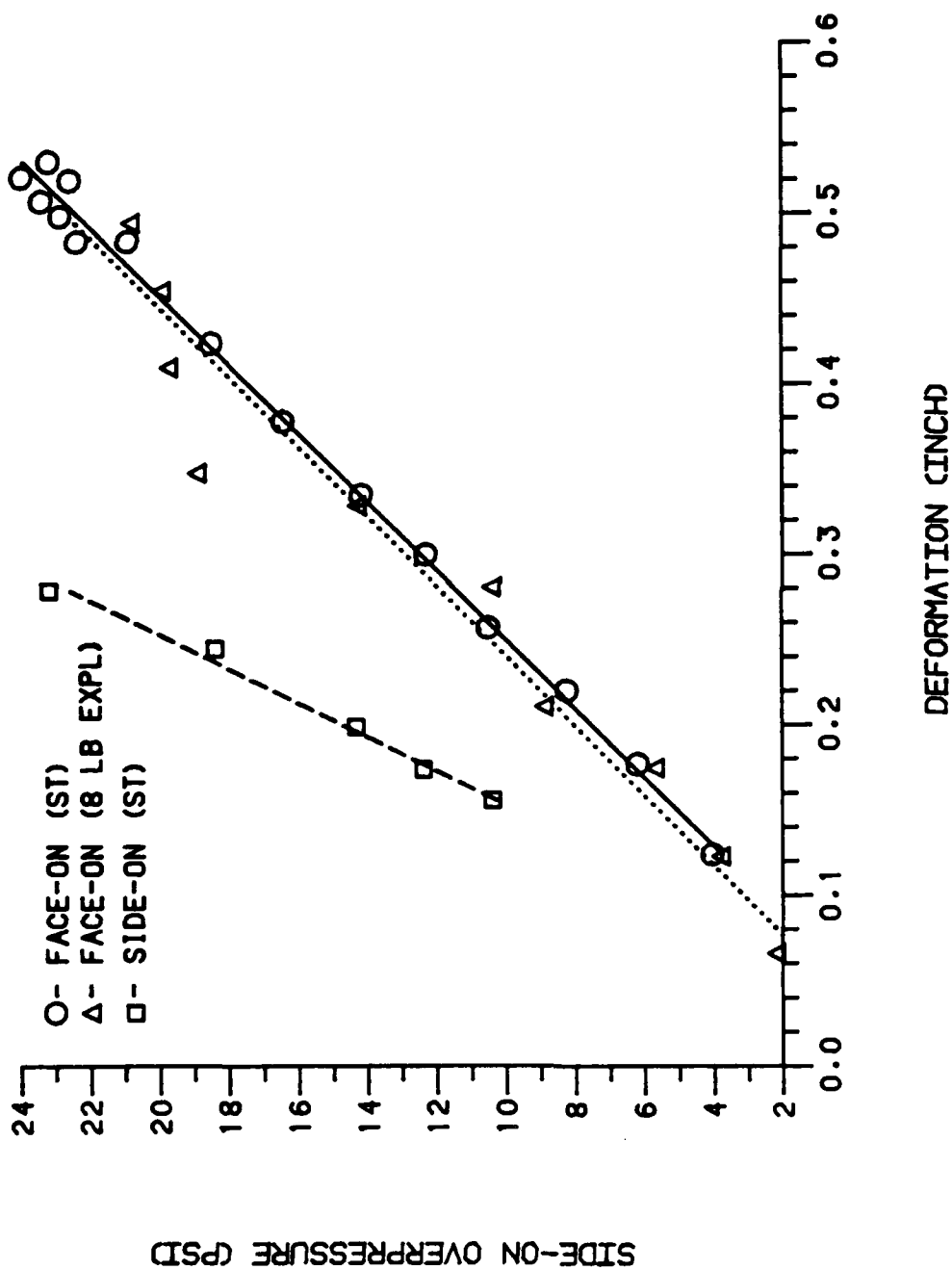


Figure 9. Calibration curves for NDDPG with .005 inch aluminum foil oriented face-on and side-on to the propagating shock

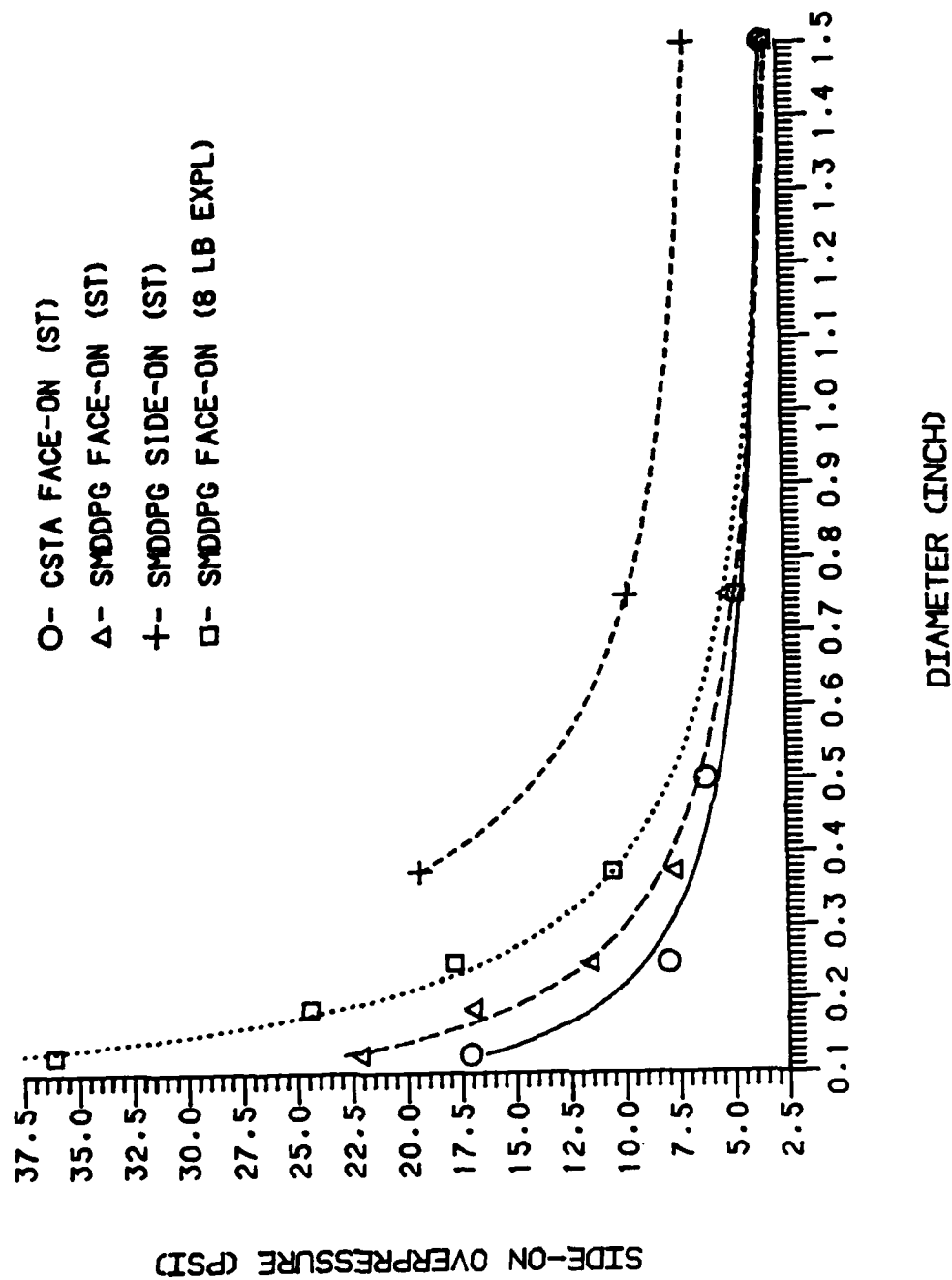


Figure 10. Calibration curves for the SMDDPG and the CSTA gage with .0005 inch foil oriented side-on and face-on to the propagating shock

TABLE 1. Rupture Overpressure for Combat Systems Testing Activity
(CSTA) Diaphragm Pressure Gage with .0005 Inch Foil

Diaphragm Ruptured*	Pressure
inch	psi
none	$P < 3.3$
1 1/2	$3.3 \leq P < 6.2$
1/2	$6.2 \leq P < 8.0$
1/4	$8.0 \leq P < 17.1$
1/8	$17.1 \leq P$

*Gage orientation is face-on with corresponding side-on overpressure recorded.

TABLE 2. Rupture Overpressure for Surface Mounted Discrete
Diaphragm Pressure Gage (SMDDPG) with .0005 Inch Foil

Diaphragm Ruptured*	Pressure
inch	psi
none	$P < 3.0$
1 1/2	$3.0 \leq P < 5.0$
3/4	$5.0 \leq P < 7.6$
3/8	$7.6 \leq P < 11.5$
1/4	$11.5 \leq P < 16.9$
3/16	$16.9 \leq P < 22.0$
1/8	$22.0 \leq P$

*Gage orientation is face-on with corresponding side-on overpressure recorded.

The SMDDPG was also oriented face-on and tests were conducted to determine the maximum, permanent, deformation in the 1 1/2 inch and 3/4 inch diameter diaphragm for .001 inch and .003 inch foil. These test values are plotted in Figure 11 and show the effects of foil diameter on permanent, maximum, deformation. The face-on orientation produces a more accurate gage and if the individual chambers are isolated, the range could be extended by using the rupture intervals whenever the 3/4 inch and 1 1/2 inch or large diaphragms rupture. Several shots against this gage oriented side-on without diaphragm rupture gave a deformed shape that was asymmetrical with the maximum permanent deformation depth being shifted from the diaphragm center. This condition also occurred for the NDDPG, shifting the maximum permanent deformation depth off the diaphragm axis of symmetry for side-on measurements. Since this shift in position of the depression is always in the direction of the shock velocity vector, one could use this characteristic to determine the direction from which a shock wave propagates when the direction is unknown.

Subsequent to the calibration in the ST, some field tests were conducted with eight pound spheres of pentolite to determine the effects of wave shape on these mechanical diaphragm gages (NDDPG's and SMDDPG's). Side-on pressure-time histories generated with explosive charges were measured with PCB type electronic gages. Typical examples of these histories are given in Figures 12a through 15 for shock strengths ranging from 3.7 psi to 64 psi. There is a decrease in positive duration as the pressure increases, hence, the impulsive load is delivered at shorter times as the pressure increases. These explosive shock data have been plotted together with the data generated from the shock tube experiments. Figures 8 and 9 show that the NDDPG is not sensitive to wave shape in the pressure range under study for face-on and side-on measurements when .003 and .005 inch foils are used. Figure 10 shows that when pressures are determined by using the rupture pressure of diaphragms, the shape of the wave and duration must be taken into account when calibrating the gage. This is not the case using foil deformation as the basis of pressure measurement, as shown in Figures 8 and 9.

No adequate apparatus was available for calibrating the quasi-static diaphragm pressure gage (QS-DPG) so the shock tube was used to approximate the peak overpressure of the long duration slow rising pressure that is generated when blast expands within enclosures. The QS-DPG was oriented such that the shock attenuating tube faced the on-coming shock, then rotated 180 degrees to determine the pressure for the same strength wave. Figure 16 shows that deformation was the same at both orientations for .005 inch foil. Since the shock was attenuated and did not affect the foil appreciably in the entrance area because of the small size, it was assumed that the high pressure gases behind the shock front that entered the front cavity of the gage deformed the foil. The fact that there was no change in deformation at both orientations

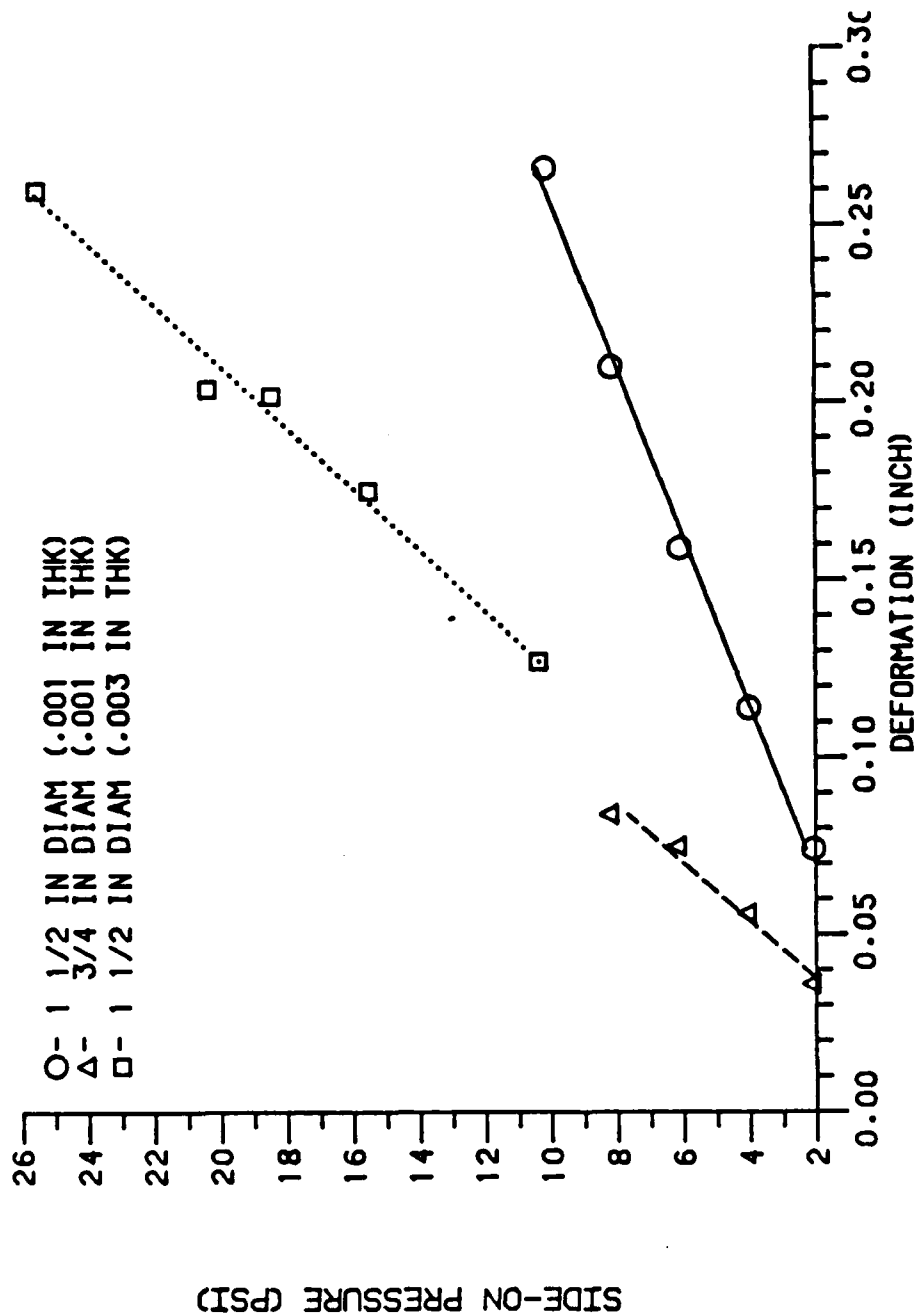


Figure 11. Calibration curves for SMDDPG 1 1/2 inch diameter and 3/4 inch diameter diaphragms oriented face-on to the propagating shock

substantiate this assumption. Only one orientation for .001 and .003 inch foil was used. In order to measure the maximum deformation in some tests, air had to be let into the rear chamber after the test. This was done by making a needle hole in the foil at the entrance (smallest diameter) or by placing a razor blade under a portion of the sealed side of the foil to relieve pressure buildup in the sealed cavity after deformation.

A large number of clean out shots were required to remove the accumulation of debris generated by the shock tube diaphragms during shock tube calibration. Provisions also had to be made to ensure debris did not impact the gages when field tests, with the eight pound Pentolite charges, were conducted.

The traditional method of assessing the effects of overpressure on exposed personnel requires estimates of the peak side-on overpressure and duration of the positive phase of the overpressure event. From the theory based on the Rankine-Hugoniot relationships, peak face-on or normally reflected pressure (P_r) can be calculated according to these relationships by:

$$P_r - P_o = (P_i - P_o) \cdot \frac{(2 + \frac{1}{\mu^2}) [\frac{(P_i + P_o)}{P_o} - 1]}{\frac{1}{\mu^2} + \frac{P_i + P_o}{P_o}} \quad (1)$$

Where

C_p - specific heat at constant pressure

C_v - specific heat at constant volume

P_i - total peak side-on pressure

P_r - total peak face-on or peak reflected pressure

P_o - ambient pressure

$$\gamma = \frac{C_p}{C_v}$$

$$\frac{1}{\mu^2} = \frac{\gamma + 1}{\gamma - 1}$$

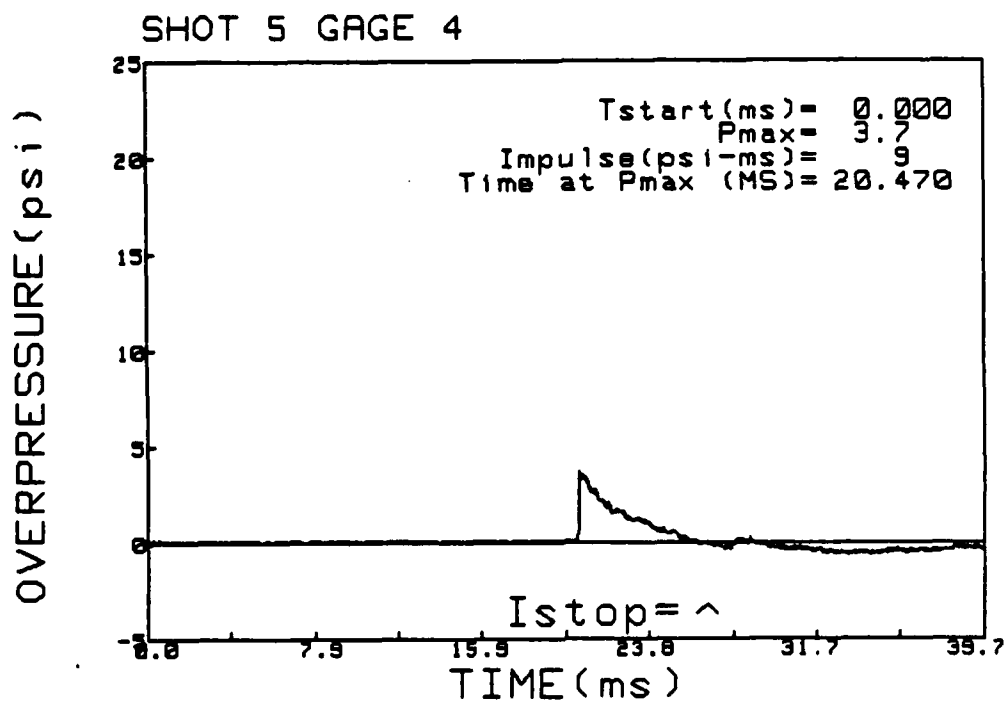


Figure 12a. Pressure-time history for 8 pounds of pentolite with a P_{max} of 3.7 psi.

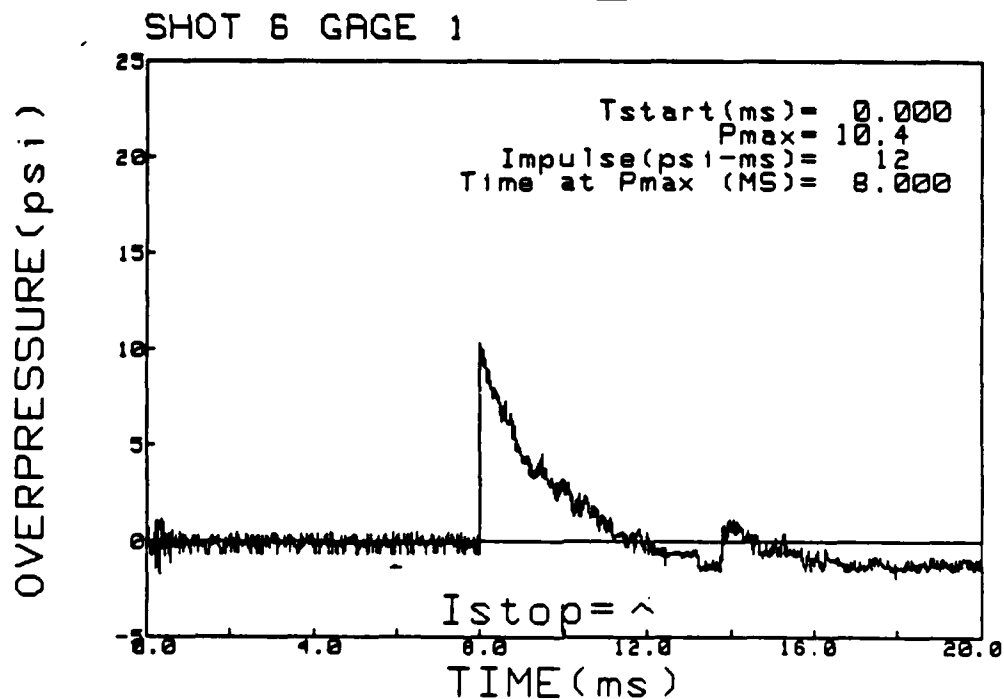


Figure 12b. Pressure-time history for 8 pounds of pentolite with a P_{max} of 10.4 psi.

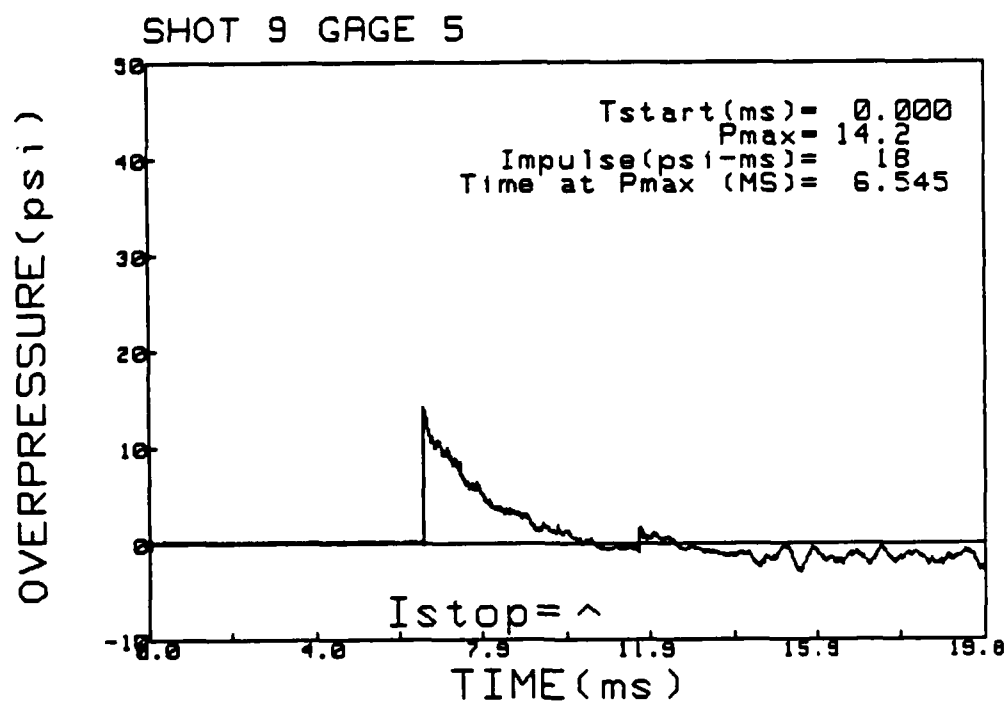


Figure 13a. Pressure-time history for 8 pounds of pentolite with a P_{max} of 14.2 psi.

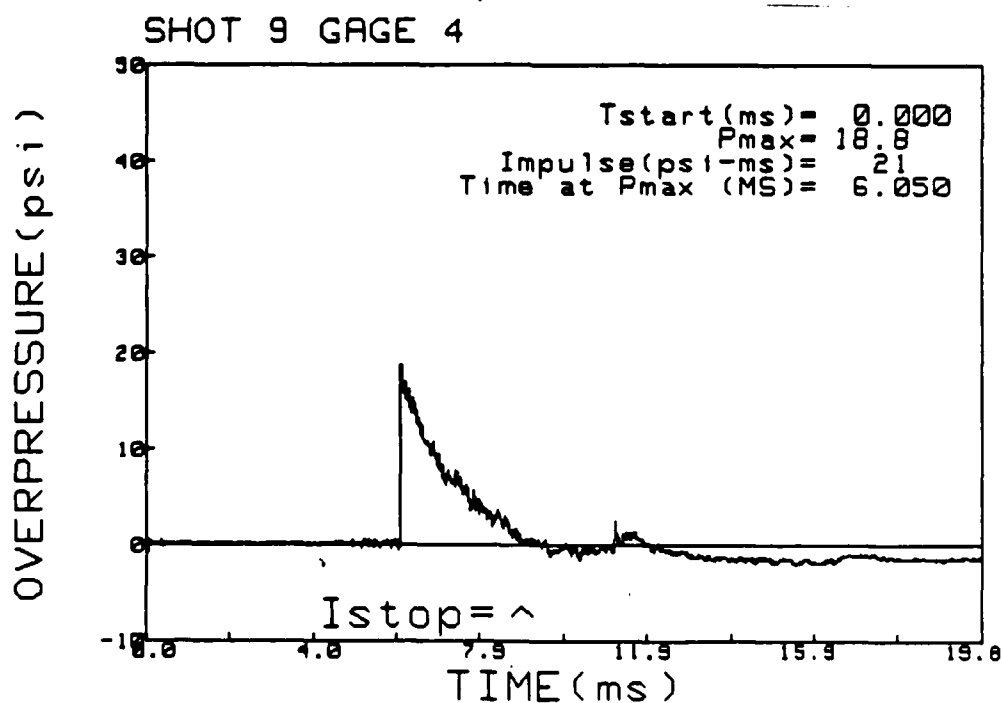


Figure 13b. Pressure-time history for 8 pounds of pentolite with a P_{max} of 18.8 psi.

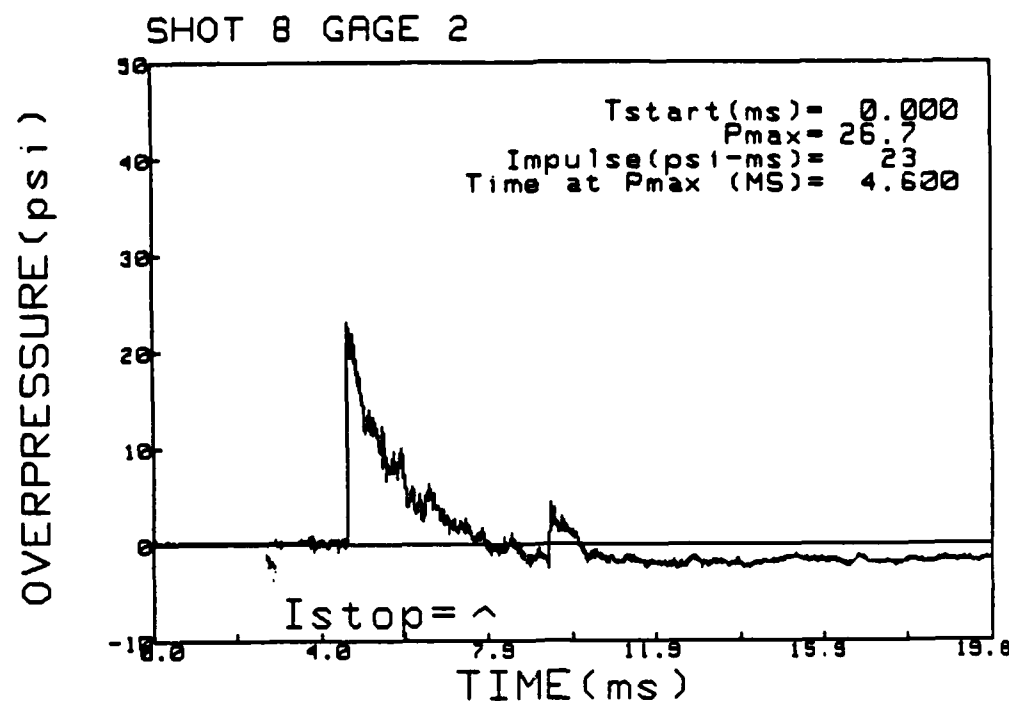


Figure 14a. Pressure-time history for 8 pounds of pentolite with a P_{max} of 26.7 psi.

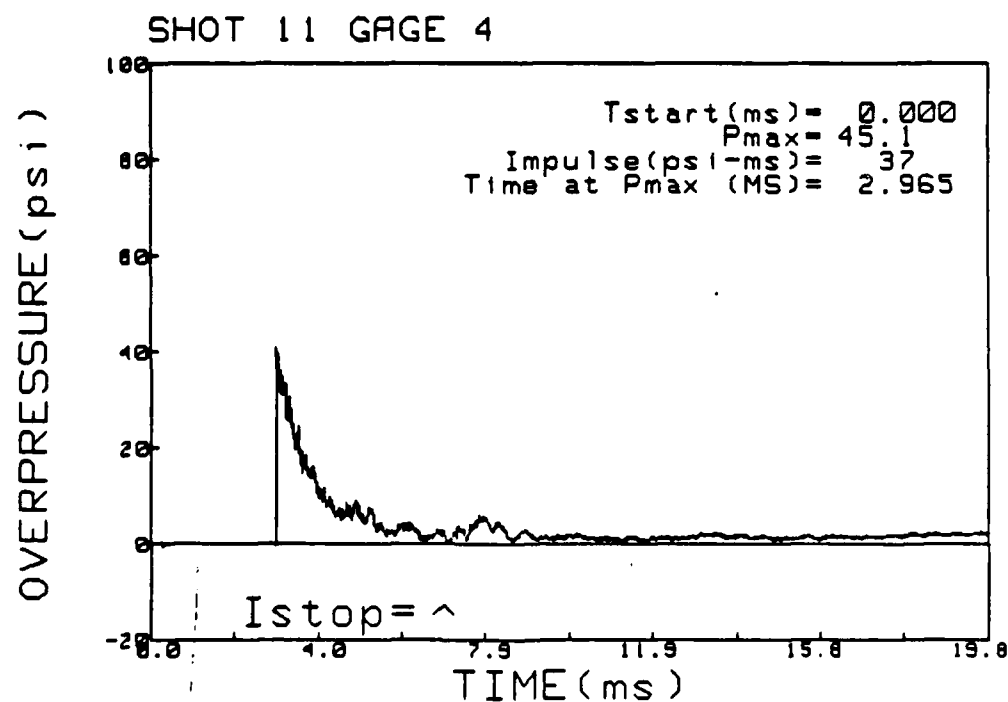


Figure 14b. Pressure-time history for 8 pounds of pentolite with a P_{max} of 45.1 psi.

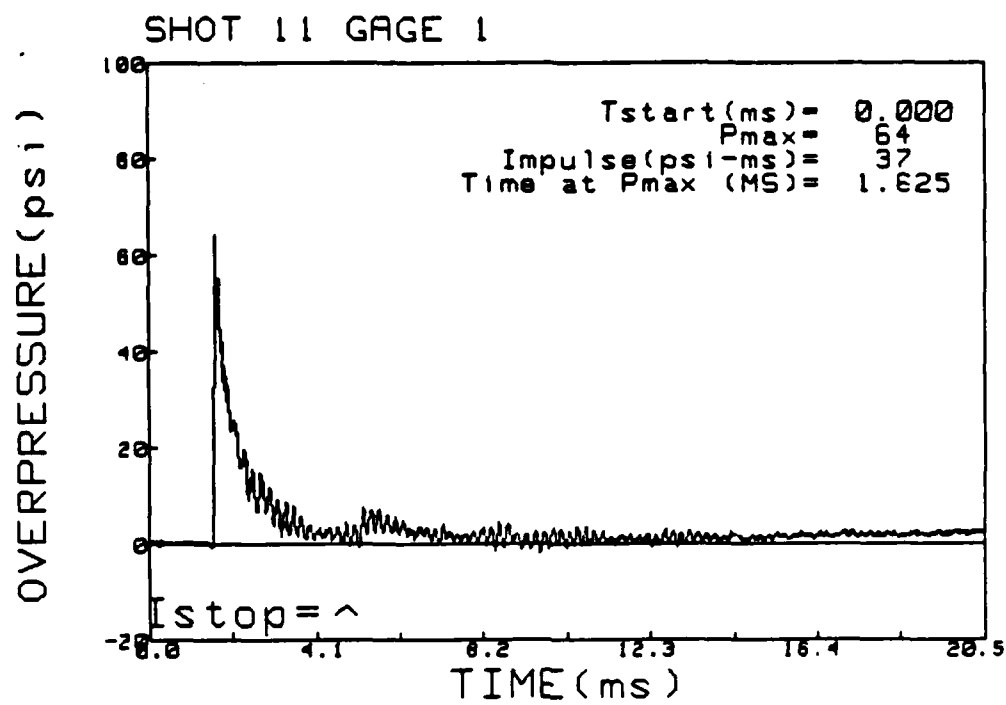


Figure 15. Pressure-time history for 8 pounds of pentolite with a Pmax of 64.0 psi.

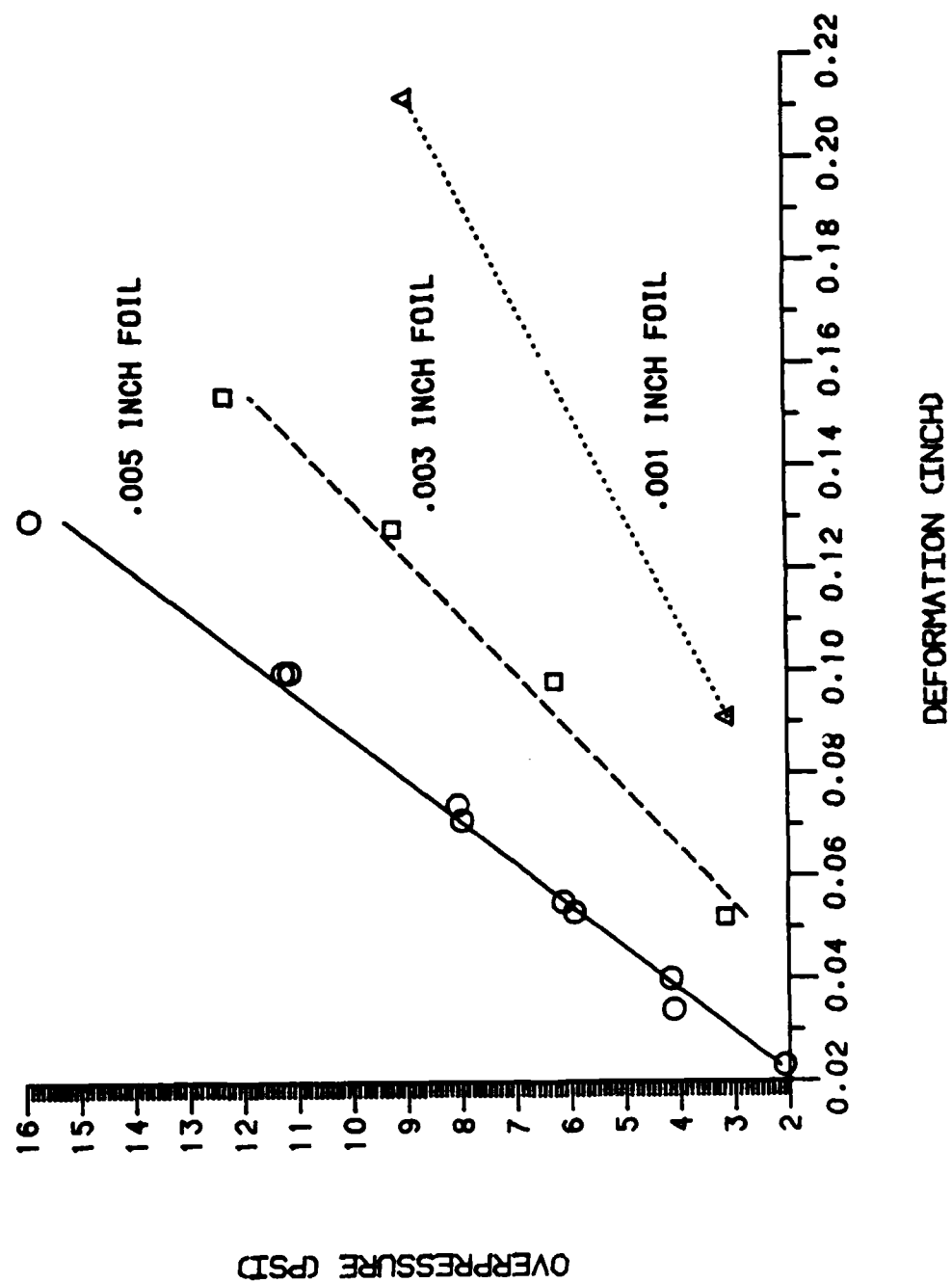


Figure 16. Calibration curves for QS-DPG

The peak face-on overpressures, $(P_F - P_0)$, computed from the peak side-on overpressures, $(P_1 - P_0)$, in equation 1 are tabulated in reference 8 and these face-on peak overpressures versus peak side-on overpressures, along with peak overpressures determined during calibration, are plotted in Figure 17; data are given for gages where the propagating shocks impact the foil face-on, 10 degree incident angle and at 30 degree incident angle. The long dash is for 0 degree (BRL RPT), the dot is for 10 degree, the short dash is for 30 degree, and the solid line is for 0 degree (ST). The pressures from reference 8 in this figure agree with those that were determined experimentally. The pressures for oblique reflections also agree. Hence, this Figure will be used to relate side-on pressure to face-on pressure in this work. One must be aware, however, that pressures for oblique impact of the shock may not always be less than those from a similar wave impinging face-on and may actually be greater. This is especially in evidence for sufficiently small angles of attack and where Mach reflection occurs.

Other important shock parameter relationships in incapacitation studies are pressure versus positive impulse, pressure versus positive duration and positive impulse versus positive duration. These relationships were obtained in the measurements made with the electronic gages when the eight pound spherical pentolite charges were used to calibrate the foil gages. These data are plotted in Figures 18, 19, and 20.

The expected pressures should determine the thickness of foil to be used in an experimental environment for the NDDPG and the QS-DPG. The NDDPG is not calibrated for multiple shocks or slow rising pressure pulses. For slow rising pressure pulses, the QS-DPG should be used.

In an environment where multiple shocks occur the NDDPG may be used if a thickness of foil is used that precludes rupture and the gage is oriented face-on to the initial shock. A small reflected shock which would not increase permanent deformation may increase the rupture length (especially for thin foil such as .0005 inch) if rupture occurs. For thicker foil (.001 to .005 inch) the rupture length should not increase significantly, if at all, for weak reflections. Therefore, one should still read the pressure from the gage if rupture occurs. It is assumed that the initial shock causes the maximum permanent deformation. If the NDDPG is mounted flush with the interior of an enclosure where shocks propagate, gage orientation is not a factor if the gage has been calibrated to measure side-on pressure.

⁸ Kingery, C.N. and Pannill, B.F.; "Parametric Analysis of the Regular Reflection of Air Blast," BRL Report No. 1249, Ballistic Research Laboratories, Aberdeen Proving Ground, MD, 1964.

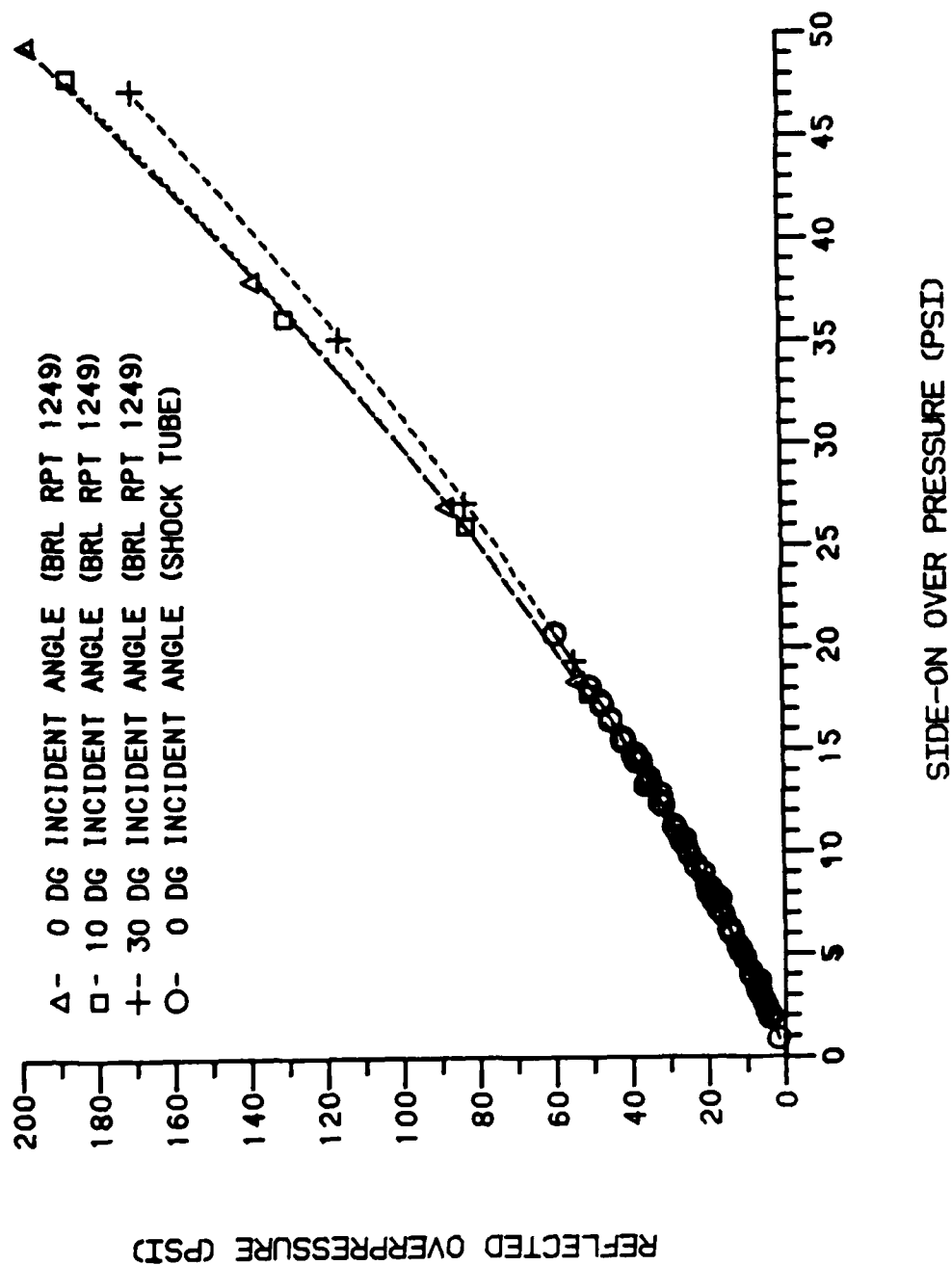


Figure 17. Reflected overpressure versus side-on overpressure.

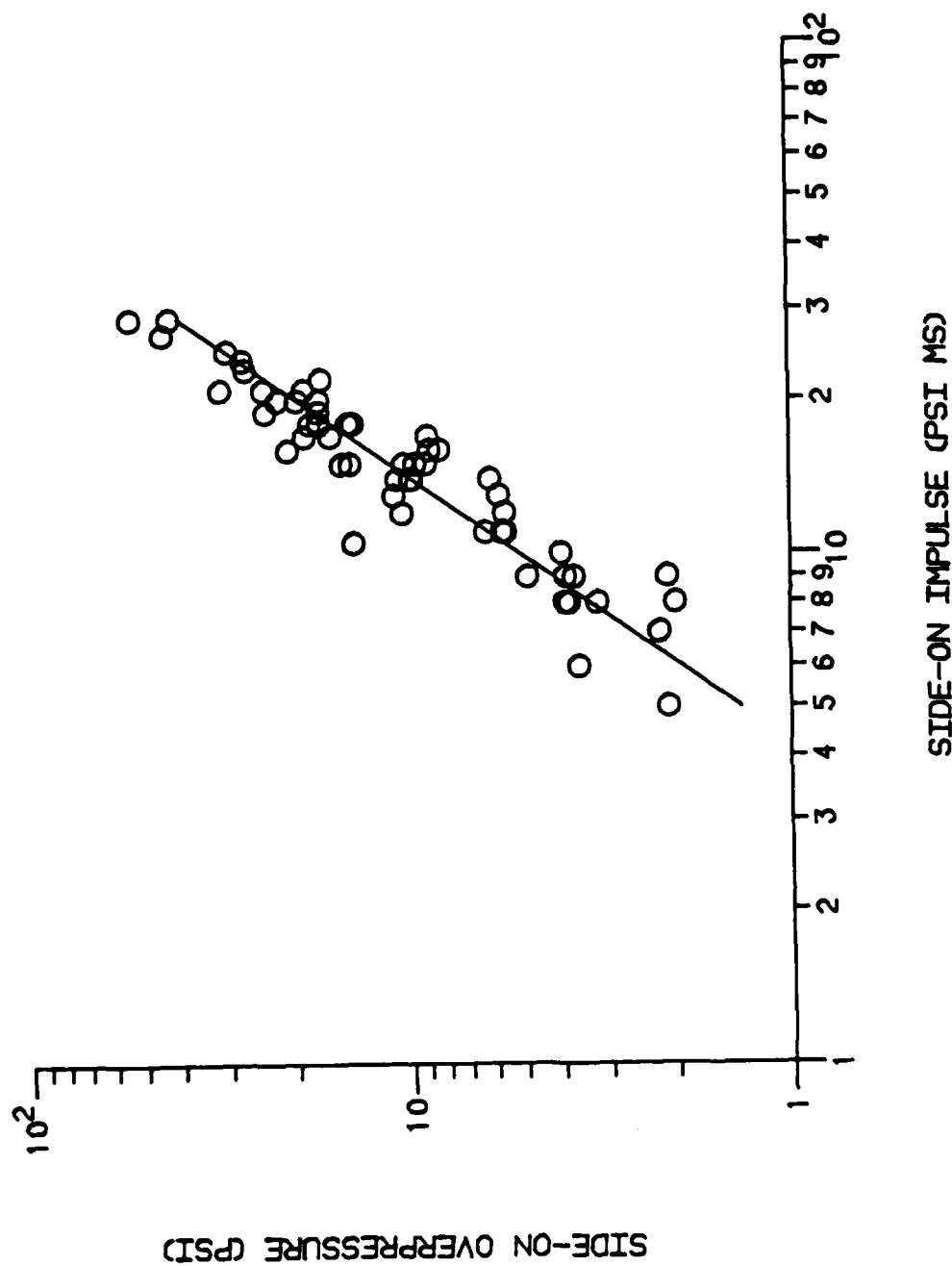
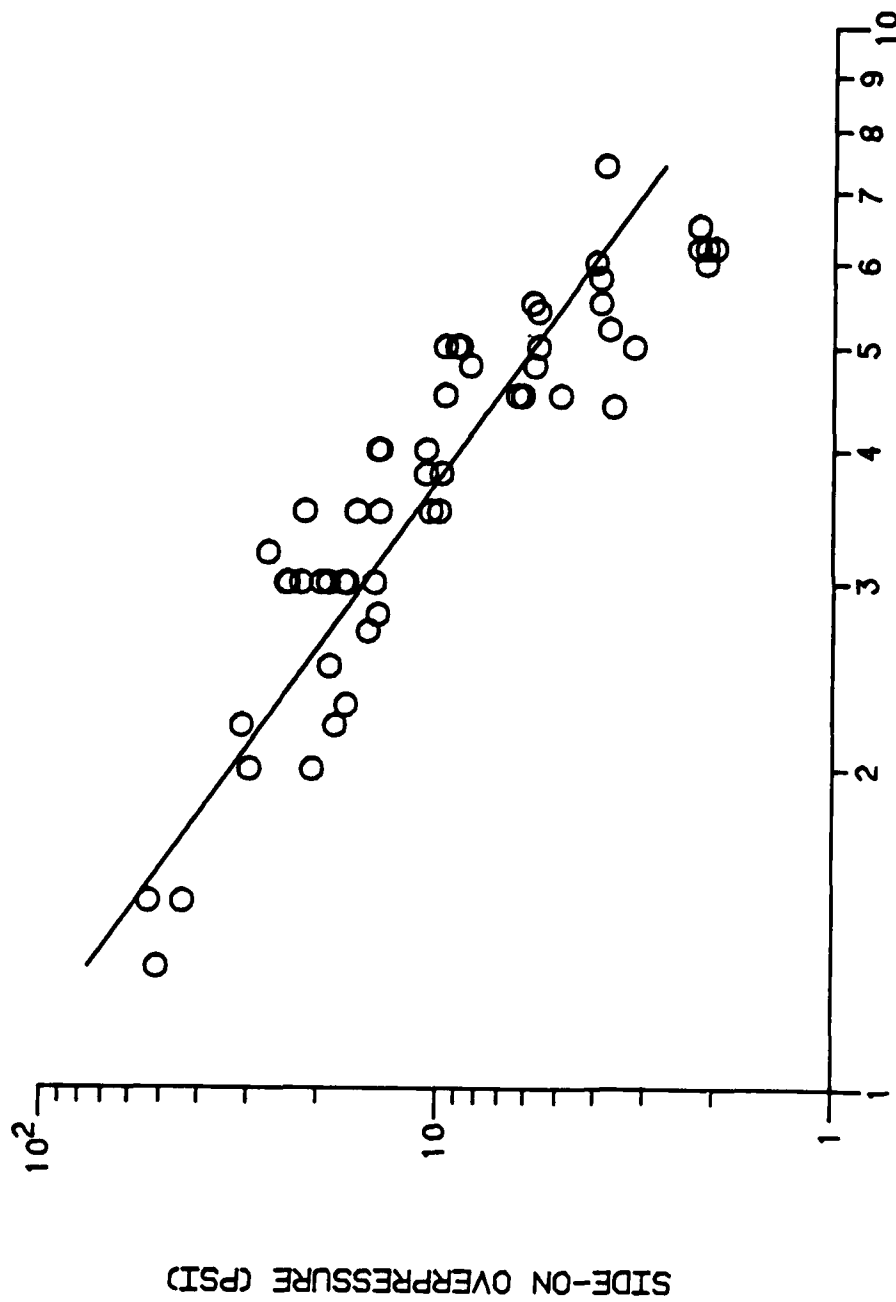


Figure 18. Side-on overpressure versus side-on impulse for 8 pounds of pentolite.



SIDE-ON DURATION (MS)

Figure 19. Side-on overpressure versus side-on duration for 8 pounds of pentolite.

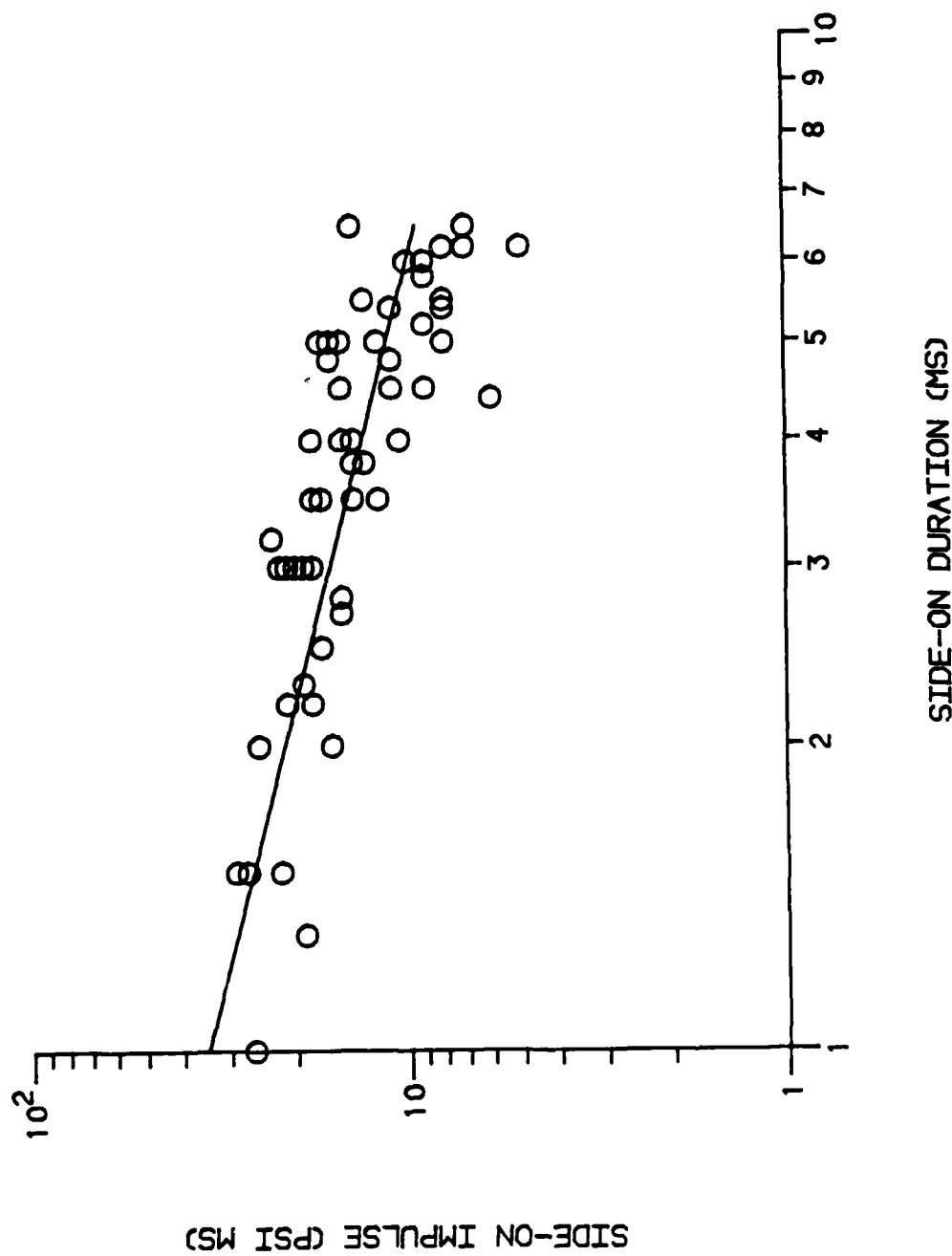


Figure 20. Side-on impulse versus side-on duration for 8 pounds of pentolite.

Even though only the QS-DPG was designed to measure pressures inside an enclosure, all gages have been used inside troop compartments to measure the pressures generated when a shaped charge impacts the compartment. The NDDPG was used for shocks and the QS-DPG was used for quasi-static pressure. In an enclosure impacted by shaped charges, usually there is no definitive evidence on the obliquity of the blast wave that propagates inside. In the absence of knowledge of the obliquity of the blast wave, it was assumed that foil gages oriented to face the impact point, when located inside an enclosure, were measuring face-on pressures and the initial shock causes the maximum deformation. Electronic transducers, when used, are mounted flush with the exposed interior. The NDDPG was placed inside the enclosure and correct orientation was impossible because the shock wave direction could only be assumed. Figure 17, however, shows that small deviations in the orientation angle causes insignificant changes in the pressure measured. Figures 21 and 22 show the deformed or ruptured foil when the gages were mounted in an enclosure impacted by a shaped charge. Several NDDPG oriented similarly to electronic transducers had measurements that were 5 to 15 percent below those measured electronically and in the range predicted by the SMDDPG and the CSTA gage. This is considered good agreement since the peaks of electronically determined pressure time histories of measurements in an enclosure impacted by a shape charge are not always clearly determined. The quasi-static pressure was approximated with the QS-DPG. The maximum pressures measured with the QS-DPG were in good agreement with the quasi-static pressure taken from the long time pressure-time curves produced by electronic transducers.

All equations generated from the LSPLIT program are given in the appendix. These equations can be used to compute the pressure whenever the deformation or rupture is known.

VI. CONCLUSION

Even though the calibration shots indicate the NDDPG is less sensitive to the pulse shape than previous diaphragm gages, we feel that the calibration pressure pulse should be similar to the pressure pulse existing in the test environment in which the gage will be used. If the initial impulsive loads delivered are similar (calibration and actual tests), it might be possible to approximate a shock duration for the NDDPG by comparison with the electronically measured pressure time histories. For CSTA type foil gages, the calibration pressure pulse should be similar to the test environment pulse. Otherwise, when a shock tube is used to calibrate the CSTA type gage and the gage is used to measure pressure pulses similar to those generated by small explosive charges, the pressure may be greatly underestimated. The importance of this factor is vitiated when the NDDPG is used to measure the pressure.

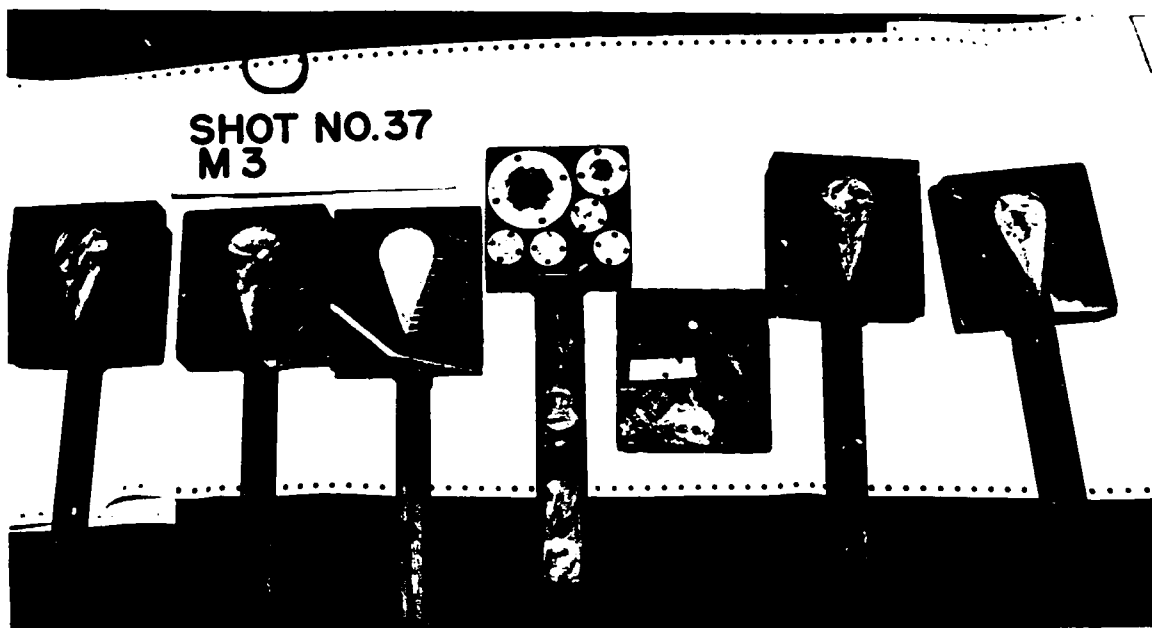


Figure 21. Diaphragm pressure gages after compartment test.

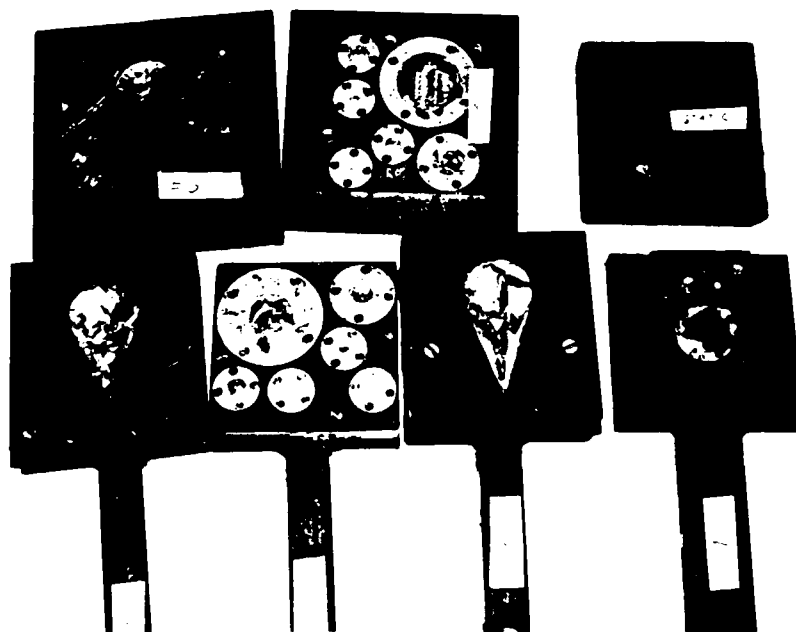


Figure 22. Diaphragm pressure gages after compartment test.

The NDDPG is a self contained, inexpensive, non-electronic gage that gives an accurate peak overpressure measure of shocks without multiple reflections that appears to be independent of the shape of the shock pressure pulse. Within the limits of the gage range, the NDDPG provides a continuous scale for the measurement of shock pressures. Moreover, the gage can still be read even if the foil ruptures, although with reduced accuracy.

The NDDPG is designed to measure fast rising pressure pulses (shocks) without multiple steps or reflections. However, if it is understood that it is the initial shock peak pressure that makes the maximum deformation or rupture used to determine the peak overpressure, the NDDPG should provide good pressure measurements in an enclosure even in the presence of such multiple pulses. The effects of orientation can be eliminated, if the gage is calibrated for side-on pressures with the gage in its test environment mounted in the walls, ceiling, or floor of the enclosure.

Experience with electronic gages has often shown that it is difficult to sort out the many peaks and spikes in pressure time histories that are produced. It's often difficult to know which represents genuine peak overpressures. Because of such difficulty in determining the actual peak overpressures from the pressure-time records of the electronic gages, located in an enclosure, the NDDPG may prove to be a valuable tool in determining the effective peak overpressure on the pressure-time record.

In the characteristic response time of 2.23 ms as set forth in Richmond's Partial Impulse Criteria,⁹ Figure 19 shows that 8 pounds of pentolite delivers an impulse of 20 psi ms. This is below the lung damage threshold of 34 psi ms. A side-on impulse of 20 psi ms corresponding to 22 psi on Figure 18 is related to a deformation of .38 inches on Figure 8 for .003 inch foil oriented side on. This analysis shows that the gage can be calibrated to give incapacitation levels without recourse to relating the deformation to pressure. This would eliminate the interpretation of peaks on suspect records.

The QS-DPG shows promise as an invaluable device for measuring quasi-static pressures. It provides accurate values of the peak overpressure for slow rising pressures in a chamber. Such pulses cause considerable damage to structures because of the high impulsive loads generated.

⁹ Richmond, D.R., et.al.; "The Relationship Between Selected Blast Wave Parameters and the Response of Mammals Exposed to Air Blast," DASA 1860, Lovelace Foundation, NM, August 1966.

The gage should be used in a non rupturing mode whenever possible, because of the ease in calibration and the repeatability of the calibration measurements.

These inexpensive, easy to use gages should always be used as back-ups when electronic transducers are used to measure pressure in a hazardous environment, thus, damage to the transducer will not result in complete failure to obtaining peak overpressure readings.

We should caution that the aluminum foil from different sources may differ in specific metal properties, and foil quality and any new batch of foil should be calibrated before using.

REFERENCES

1. Read, W.T.; "Calibration and Use of Diaphragm Blast Meters," NDRC Report No. A392 (OSRD Report No. 6363), Division 2, National Defense Research Committee, Washington, D.C., 1945.
2. Dresner, Lawrence; "Motion of Elasto-Plastic Membranes Under Shock Loading," Journal Of Applied Physics, Volume 41, No 5, 1970.
3. Meszaros, Julius; "Determination of Mach Region Blast Pressure with Foil Meters," Operation Greenhouse, Scientific Director Report WT-55 Annex 1.6, Part III, Section 2, Ballistic Research Laboratories, Aberdeen Proving Ground, MD, 1951 (C).
4. Manweiler, R.W.; Chester, C.V.; and Kearney, C.H.; "Measurements of Shock Over-Pressures in Air by a Yielding Foil Membrane Blast Gage," ORNL Report 4863, Oak Ridge National Laboratory, Oak Ridge, Tennessee, September 1973.
5. Hudson, G.E.; "A Theory of the Dynamic Deformation of a Thin Diaphragm," Journal of Applied Physics, Volume 22, Number 1, January 1951.
6. Sachs, George; Epsey, George; and Kasik, G.P.; "Circular Bulging of Aluminum-Alloy Sheets at Room and Elevated Temperature," ASME, January-December 1946.
7. Goodman, Henry J.; "Aerodynamic and Frequency Dependent Errors in Air Blast Gages," BRL Report 1345, Ballistic Research Laboratories, APG, MD, October 1966.
8. Kingery, C.N. and Pannill, B.F.; "Parametric Analysis of the Regular Reflection of Air Blast," BRL Report No. 1249, Ballistic Research Laboratories, APG, MD, 1964.
9. Richardson, D.R., et. al.; "The Relationship Between Selected Blast Wave Parameters and the Response of Mammals Exposed to Air Blast," DASA 1860, Lovelace Foundation, Albuquerque, NM, August 1966.

APPENDIX - EQUATIONS

APPENDIX - EQUATIONS

No - 1a

Gage Type - NDDPG

Foil Thickness - .0005 inch

Orientation - Face-on

Measurement Type - Shock Deformation (A-M) / Shock Tube

See Figure 6.

$$P_i = .402 + 6.84DM \text{ psi} \quad (A-1)$$

No - 1b

Gage Type - NDDPG

Foil Thickness - .0005 inch

Orientation - Face-on

Measurement Type - Shock Rupture (A-R) / Shock Tube

See Figure 6.

$$P_i = 2.80 + .243DR \text{ psi} \quad (A-2)$$

No - 2a

Gage Type - NDDPG

Foil Thickness - .001 inch

Orientation - Face-on

Measurement Type - Shock Deformation (A-M) / Shock Tube

See Figure 7.

$$P_i = -.355 + 13.2DM \text{ psi} \quad (A-3)$$

No - 2b

Gage Type - NDDPG

Foil Thickness - .001 inch

Orientation - Face-on

Measurement Type - Shock Rupture (A-R) / Shock Tube

See Figure 7.

$$P_i = 3.34 + .598DR \text{ psi} \quad (A-4)$$

No - 3a

Gage Type - NDDPG

Foil Thickness - .003 inch

Orientation - Face-on

Measurement Type - Shock Deformation (A-M) / Shock Tube

See Figure 8.

$$P_i = -1.64 + .346DM \text{ psi} \quad (A-5)$$

No - 3b

Foil Thickness - .003 inch

Orientation - Side-on

Measurement Type - Shock Deformation (A-M) / Shock Tube

See Figure 8.

$$P_i = -2.81 + 61.2DM \text{ psi} \quad (A-6)$$

No - 3c

Foil Thickness - .003 inch

Orientation - 10 Degree Incident

Measurement Type - Shock Deformation (A-M) / Explosive

See Figure 8.

$$P_i = -1.46 + 32.8DM \text{ psi} \quad (A-7)$$

No - 3d

Gage Type - NDDPG

Foil Thickness .003 inch

Orientation - 30 Degree Incident

Measurement Type - Shock Deformation (A-M) / Shock Tube

See Figure 8.

$$P_i = -1.76 + 36.1DM \text{ psi} \quad (A-8)$$

No - 3e

Gage Type - NDDPG

Foil Thickness - .003 inch

Orientation - Face-on

Measurement Type - Shock Deformation (A-M) / Explosive

See Figure 8.

$$P_i = -1.28 + 32.8DM \text{ psi} \quad (A-9)$$

No - 3f

Gage Type - NDDPG

Foil Thickness - .003 inch

Orientation - Side-on

Measurement Type - Shock Deformation (A-M) / Explosive

See Figure 8.

$$P_i = -3.92 + 68.9DM \text{ psi} \quad (A-10)$$

No - 4a

Gage Type - NDDPG

Foil Thickness - .005 inch

Orientation - Face-on

Measurement Type - Shock Deformation (A-M) / Shock Tube

See Figure 9.

$$P_i = -2.37 + 49.4DM \text{ psi} \quad (A-11)$$

No - 4b

Gage Type - NDDPG

Foil Thickness .005 inch

Orientation - Face-on

Measurement Type - Shock Deformation (A-M) / Explosive

See Figure 9.

$$P_i = -1.74 + 48DM \text{ psi} \quad (A-12)$$

No - 4c

Gage Type - NDDPG

Foil Thickness - .0005 inch

Orientation - Side-on

Measurement Type - Shock Deformation (A-M) / Shock Tube

See Figure 9.

$$P_i = -5.30 + 99.8DM \text{ psi} \quad (A-13)$$

No - 5a

Gage Type - CSTA

Foil Thickness - .0005 inch

Orientation - Face-on

Measurement Type - Shock Rupture (A-R) / Shock Tube

See Figure 10.

$$P_i = 3.9DR^{-.443e^{(A-1180DR^2)}} \text{ psi} \quad (A-14)$$

No - 5b

Gage Type - SMDDPG

Foil Thickness - .0005 inch

Orientation - Face-on

Measurement Type - Shock Rupture (A-R) / Shock Tube

See Figure 10.

$$P_i = 3.92DR^{-1669e^{(A-98320DR^2)}} \text{ psi} \quad (A-15)$$

No - 5c

Gage Type - SMDDPG

Foil Thickness - .0005 inch

Orientation - Face-on

Measurement Type - Shock Rupture (A-R) / Shock Tube

See Figure 10.

$$P_i = 4.14DR^{-.831e^{(A-1180DR^2)}} \text{ psi} \quad (A-16)$$

No - 5d

Gage Type - SMDDPG

Foil Thickness - .0005 inch

Orientation - Side-on

Measurement Type - Shock Rupture (A-R) / Shock Tube

See Figure 10.

$$P_i = 8.03DR^{-.557e^{(A-.3+4.4DR^2)}} \text{ psi} \quad (\text{A-17})$$

No - 6a

Gage Type - SMDDPG (A-ithout rupture)

Foil Thickness - .001 inch in 1 1/2 inch diameter

Orientation - Face-on

Measurement Type - Shock Deformation (A-M) / Shock Tube

See Figure 11.

$$P_i = -.832 + 42.0DM \text{ psi} \quad (\text{A-18})$$

No - 6b

Gage Type - SMDDPG (A-ithout rupture)

Foil Thickness - .001 inch in 3/4 inch diameter

Orientation - Face-on

Measurement Type - Shock Deformation (A-M) / Shock Tube

See Figure 11.

$$P_i = -4.26 + 115DM \text{ psi} \quad (\text{A-19})$$

No - 6c

Gage Type - SMDDPG (A-ithout rupture)

Foil Thickness - .003 inch in 1 1/2 inch diameter

Orientation - Face-on

Measurement Type - Shock Deformation (A-M) / Shock Tube

See Figure 11.

$$P_i = -2.57 + 122DM \text{ psi} \quad (\text{A-20})$$

No - 7a

Gage Type - QS-DPG

Foil Thickness - .001 inch

Measurement Type - Shock Deformation (A-M) / Quasi-Static Pressure

See Figure 16.

$$P_{qs} = -1.26 + 47DM \text{ psi} \quad (A-22)$$

No - 7b

Gage Type - QS-DPG

Foil Thickness - .003 inch

Measurement Type - Shock Deformation (A-M) / Quasi-Static Pressure

See Figure 16.

$$P_{qs} = -1.84 + 88.5DM \text{ psi} \quad (A-23)$$

No - 7c

Gage Type - QS-DPG

Foil Thickness - .005 inch

Measurement Type - Shock Deformation (A-M) / Quasi-Static Pressure

See Figure 16.

$$P_{qs} = -.642 + 122DM \text{ psi} \quad (A-24)$$

No - 8a

Gage Type - Electronic

Orientation - Face-on and Side-on

Measurement Type - Shock Pressure-Time Histories (A-BRL Report 1249)

See Figure 17.

$$P_r = -1.43 + 2.44P_i + .0313P_i^2 \text{ psi} \quad (A-25)$$

NO - 8b

Gage Type - Electronic

Orientation - Face-on and Side-on

Measurement Type - Shock Pressure-Time Histories (A-BRL Report 1249)

See Figure 17.

$$P_r = -1.54 + 2.47P_i + .030P_i^2 \text{ psi} \quad (\text{A-26})$$

No - 8c

Gage type - Electronic

Orientation - Face-on and Side-on

Measurement Type - Shock Pressure-Time Histories (A-BRL Report 1249)

See Figure 17.

$$P_r = -1.04 + 2.39P_i + .025P_i^2 \text{ psi} \quad (\text{A-27})$$

No - 8d

Gage Type - Electronic

Orientation - Side-on

Measurement Type - Shock Pressure-Time Histories and Computed Shock Pressures

See Figure 17.

$$P_r = -.297 + 2.19P_i + .034P_i^2 \text{ psi} \quad (\text{A-28})$$

No - 9

Gage Type - Electronic

Orientation - Side-on

Measurement Type - Shock Pressure-Time Histories / Explosive

See Figure 19.

$$P_i = .062I^{1.92} \text{ psi} \quad (\text{A-29})$$

No - 10

Gage Type - Electronic

Orientation - Side-on

Measurement Type - Shock Pressure-Time Histories / Explosive

See Figure 20.

$$P_i = 125T^{-1.92} \text{ psi} \quad (\text{A-30})$$

No - 11

Gage Type - Electronic

Orientation - Side-on

Measurement Type - Shock Pressure-Time Histories / Explosive

See Figure 21.

$$I_i = 34.6T^{-.697} \text{ psi ms} \quad (\text{A-31})$$

LIST OF SYMBOLS

CSTA	- Combat Systems Testing Activity
C_p	-specific heat at constant pressure
C_v	-specific heat at constant volume
DG	- degree
DIAM	- diameter (inch)
DM	- deformation depth (inch)
DR	- rupture length (graduations) beginning with graduation at maximum diameter on gage housing
ms	- millisecond
NDDPG	- non-discrete diaphragm pressure gage
P	- overpressure of the SMDDPG or CSTA gage (psi)
P_i	- total side-on peak pressure (psi)
P_{max}	- electronically measured side-on peak overpressure (psi)
P_o	- ambient pressure (psi)
P_r	- total face-on or normally reflected pressure (psi)
psi	- pounds per square inch
QS-DPG	- quasi-static diaphragm overpressure gage
RPT	- report
SCALE	- graduations on front of gage housing that are used to measure the rupture length
SMDDPG	- surface mounted discrete diaphragm pressure gage
ST	- shock tube
THK	- thick
γ	- $\frac{C_p}{C_v}$
μ^2	- $\frac{\gamma - 1}{\gamma + 1}$

DISTRIBUTION LIST

<u>No. of</u> <u>Copies</u>	<u>Organization</u>	<u>No. of</u> <u>Copies</u>	<u>Organization</u>
12	Administrator Defense Technical Info Center ATTN: DTIC-DDA Cameron Station Alexandria, VA 22304-6145	1	Director U.S. Army Air Mobility Research and Development Command Ames Research Center Moffett Field, CA 94035
1	HQDA ATTN: DAMA-ART-M Washington, DC 20310	1	Commander U.S. Army Communications - Electronics Command ATTN: AMSEL-ED Fort Monmouth, NJ 07703
1	Commander U.S. Army Materiel Command ATTN: AMCDE-DW 5001 Eisenhower Avenue Alexandria, VA 22333	1	Commander U.S. Army Electronics Research and Development Command Technical Support Activity ATTN: DELSD-L Fort Monmouth, NJ 07703-5301
1	Commander Armament R&D Center U.S. Army AMCCOM ATTN: SMCAR-TSS Dover, NJ 07801-5001	1	Commander U.S. Army Missile Command ATTN: AMSMI-R Redstone Arsenal, AL 35898-5241
1	Commander Armament R&D Center U.S. Army AMCCOM ATTN: SMCAR-TDC Dover, NJ 07801-5001	1	Commander U.S. Army Missile Command ATTN: AMSMI-YDL Redstone Arsenal, AL 35898-5241
1	Director Benet Weapons Laboratory Armament R&D Center U.S. Army AMCCOM ATTN: SMCAR-LCB-TL Watervliet, NY 12189	1	Commander U.S. Army Mobility Equipment Research & Development Command ATTN: DRDME-WC Fort Belvoir, VA 22060
1	Commander U.S. Army Armament Munitions & Chemical Command ATTN: SMCAR-ESP-L Rock Island, IL 61299	1	Commander U.S. Army Mobility Equipment Command 4300 Goodfellow Blvd St. Louis, MO 63120
1	Commander U.S. Army Aviation Research and Development Command ATTN: AMSAV-E 4300 Goodfellow Blvd St. Louis, MO 63120	1	Commander U.S. Army Tank Automotive Command ATTN: AMSTA-TSL Warren, MI 48397-5000

DISTRIBUTION LIST

<u>No. of Copies</u>	<u>Organization</u>	<u>No. of Copies</u>	<u>Organization</u>
1	Director U.S. Army TRADOC Systems Analysis Activity ATTN: ATAA-TEM White Sands Missile Range, NM 88002	1	Commander U.S. Army Armor Center ATTN: ATZK-M1 Fort Knox, KY 40121
1	Director U.S. Army TRADOC Systems Analysis Activity ATTN: ATAA-TFB White Sands Missile Range, NM 88002	1	Commander U.S. Army Field Artillery School Fort Sill, OK 73503
1	Director U.S. Army TRADOC Systems Analysis Activity ATTN: ATAA-SL White Sands Missile Range, NM 88002	1	Commander U.S. Army Development and Employment Agency ATTN: MODE-TED-SAB Fort Lewis, WA 98433-5000
1	Commander U.S. Army Training & Doctrine Cmd ATTN: ATCD Fort Monroe, VA 23351	3	Commander Naval Weapons Center ATTN: Code 3917 (Mr. Mel Keith) (Mr. Rex Randolph) (Mr. Jack Bates) China Lake, CA 93555-6001
1	Commander U.S. Army Training & Doctrine Cmd ATTN: ATCD-M Fort Monroe, VA 23351	2	Commander Marine Corps Development & Education Command ATTN: Firepower Division Plans & Studies Div Quantico, VA 22134
1	Commandant U.S. Army Infantry School ATTN: ATSH-CD-CSO-OR Fort Benning, GA 31905	1	Commander U.S. Marine Corps ATTN: APW Washington, DC 20380
1	Commander U.S. Army Armor Center ATTN: ATZK-CG Fort Knox, KY 40121	1	AFATL/DLYV ATTN: James Flint Eglin AFB, FL 32542
1	Commander U.S. Army Armor Center ATTN: ATZK-CD Fort Knox, KY 40121	1	AFWL/SUL Kirtland AFB, NM 87117
		1	Air Force Armament Laboratory ATTN: AFATL/DLODL Eglin AFB, FL 32542-5000

DISTRIBUTION LIST

<u>No. of Copies</u>	<u>Organization</u>	<u>No. of Copies</u>	<u>Organization</u>
1	AAI Corp. York Road & Indsutry Lane Cockeysville, MD 21030	1	Genesis Consultants LTD, Inc. ATTN: Mr. Adwin C. Hodges 715 Kyle Drive Arlington, TX 76011-2360
1	Abex Corp. Research Center Mahwah, NJ 07430	1	General Dynamics P.O. Box 2507 Pomona, CA 91766
1	Aerojet Ordnance Co. 9236 East Hall Road Downey, CA 90241	1	Honeywell Corp. ATTN: G. Robinson 600 2nd Street, NE Hopokins, MN 55343
1	AVCO systems Division 201 Lowell Street Wilmington, MA 01887	1	Honeywell Defense Systems Division ATTN: John R. Post 5640 Smetona Drive Minnetonka, MN 55343
1	Battelle Institute ATTN: Dr. B. Trott 505 King Avenue Columbus, OH 43201	1	Institute for Defense Analysis ATTN: Dr. Lowell Tonnesson 1801 Beauregard Street Alexandria, VA 22311
1	BMV Corp ATTN: Mike Mengelkamp P.O. Box 1512 York, PA 17405	1	Lawrence Livermore National Laboratory P.O. Box 808 Livermore, CA 94550
1	Beoing Aerospace Co. Seattle, WA 84124	1	Los Alamos National Laboratory P.O. Box 1663 Main Station 5000 Los Alamos, NM 87544
1	California Research & Tech., Inc. ATTN: D.L. Orphal Livermore, CA 94550	1	Martin Marietta Aerospace P.O. Box 5837 M-P-276 Orlando, FL 32805
1	Chamberlain Mfg. Corp. Research & Development Div. 550 Esther Street Waterloo, IA 50704	1	Mason & Hanger-Silas Mason, Co., Inc. Iowa Army Ammunition Plant Middletown, IA 52638
2	Denver Research Institute University Park Station ATTN: R. Recht Gale W. Weeding Denver, CO 80200	1	New Mexico Institute of Mining and Technology ATTN: TERA Group (Mr. Pat Buckley) (Mr. Phil McLain) Socorro, NM 87801
1	Ford Aerospace Communications Corp. 2 Aeronutronics Division Newport Beach, CA 92663		

DISTRIBUTION LIST

<u>No. of Copies</u>	<u>Organization</u>	<u>No. of Copies</u>	<u>Organization</u>
1	Nuclear Metals, Inc. 2229 Main Street Concord, MA 01742	1	Cdr, USATECOM ATTN: AMSTE-TO-F
1	Olin Corp. P.O. Drawer G Marion, IL 62959	3	Cdr, CRDC, AMCCOM ATTN: SMCCR-RSP-A SMCCR-MU SMCCR-SPS-IL
1	Physics International 2700 Merced Street San Leandro, CA 94577	4	Cdr, CSTA ATTN: STECS-AS-MV
1	Raytheon Co. Hartwell Road Bedford, MA 01730	4	Dir, USABRL ATTN: SLCBR-VL (Mr. David Rigotti) SLCBR-VL-S (Dr. Albert Rainis) SLCBR-VL-L (Mr. Orlando Johnson) 2 cy
1	Sandia National Laboratories Albuquerque, NM 87115		
1	Southwest Research Institute ATTN: Dr. William E. Baker 6220 Culebra road P.O. Box 28510 San Antonio, TX 78284		
1	Talley Defense Systems ATTN: Tom Simcox 3322 S. Memorial Parkway Huntsville, AL 35801		
1	Tracor MBA 1911 N. Fort Myer Drive Suite 302 Arlington, VA 22209		
1	H.P. White Laboratory 3114 Scarborough Road Street, MD 21554		
	<u>Aberdeen Proving Ground</u>		
3	Dir, USAMSAA ATTN: AMXSJ-J (Mr. John Blomquist) (Mr. Harvey Lee) AMXSJ-C (Mr. James O'Bryon)		

USER EVALUATION SHEET/CHANGE OF ADDRESS

This Laboratory undertakes a continuing effort to improve the quality of the reports it publishes. Your comments/answers to the items/questions below will aid us in our efforts.

1. BRL Report Number _____ Date of Report _____

2. Date Report Received _____

3. Does this report satisfy a need? (Comment on purpose, related project, or other area of interest for which the report will be used.) _____

4. How specifically, is the report being used? (Information source, design data, procedure, source of ideas, etc.) _____

5. Has the information in this report led to any quantitative savings as far as man-hours or dollars saved, operating costs avoided or efficiencies achieved, etc? If so, please elaborate. _____

6. General Comments. What do you think should be changed to improve future reports? (Indicate changes to organization, technical content, format, etc.) _____

CURRENT ADDRESS	_____
	Name

	Organization
_____	Address
_____	City, State, Zip

7. If indicating a Change of Address or Address Correction, please provide the New or Correct Address in Block 6 above and the Old or Incorrect address below.

OLD ADDRESS	_____
	Name

	Organization
_____	Address
_____	City, State, Zip

(Remove this sheet along the perforation, fold as indicated, staple or tape closed, and mail.)

----- FOLD HERE -----

Director
U.S. Army Ballistic Research Laboratory
ATTN: SLCBR-DD-T
Aberdeen Proving Ground, MD 21005-5066



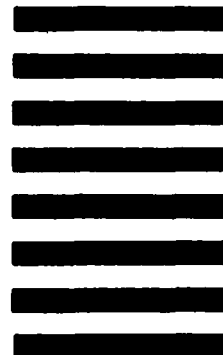
NO POSTAGE
NECESSARY
IF MAILED
IN THE
UNITED STATES

OFFICIAL BUSINESS
PENALTY FOR PRIVATE USE, \$300

BUSINESS REPLY MAIL
FIRST CLASS PERMIT NO 12062 WASHINGTON, DC

POSTAGE WILL BE PAID BY DEPARTMENT OF THE ARMY

Director
U.S. Army Ballistic Research Laboratory
ATTN: SLCBR-DD-T
Aberdeen Proving Ground, MD 21005-9989



----- FOLD HERE -----

END

5-87

DTIC